TRI-REFORMING OF NATURAL GAS FOR HYDROGEN PRODUCTION

A Dissertation

Submitted on partial fulfilment of the requirement

for the award of degree of

Masters in Technology

in

Environment Science & Technology

Submitted by

Himanshu Sharma

601601011

Under the Guidance of

Dr. Amit Dhir

Associate Professor

Mr. Rajesh M Badhe

DGM, Alternative Energy,

THAPAR INSTITUTE
OF ENGINEERING & TECHNOLOGY
(Deemed to be University)

SCHOOL OF ENERGY AND ENVIRONMENT

THAPAR INSTITUTE OF ENGINEERING & TECHNOLOGY, PATIALA

(Declared as Deemed-to-be-University u/s 3 of the UGC Act, 1956)

June 2018

DECLARATION CUM CERTIFICATE

I hereby declare that the project work entitled "**Tri-Reforming of Natural Gas for Hydrogen Production**" is an authentic record of my own work carried out at R&D Centre, IOCL Faridabad, as requirements of one-year project internship for the award of degree of M.Tech. (Environment Science & Technology), Thapar Institute of Engineering & Technology, Patiala, under the guidance of Mr. Rajesh M Badhe and Dr. Amit Dhir, during June 2017 to June 2018

Himanshu Sharma

Date: 23/07/2018 601601011

Certified that the above statement made by the student is correct to the best of our knowledge and belief.

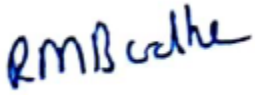

Dr. Amit Dhir
Associate Professor

Mr. Rajesh M Badhe
DGM, Alternative Energy

Acknowledgment

I am using this opportunity to express my gratitude to everyone who supported me throughout the course of this Internship. I am thankful for their aspiring guidance, invaluable constructive criticism, and friendly advice during the project work.

I express earnest gratitude to **Indian Oil Corporation Research and Development Centre, Faridabad** for giving me this opportunity. I sincerely thank **Mr. Rajesh M Badhe, Deputy General Manager (AE), IOCL R&D, Dr. Amit Dhir, Associate Professor(SEE),** and **Mr. G Sivarama Krishna, Senior Research Manager (AE), IOCL R&D** for giving me full support and guidance. This endeavor wouldn't have been fruitful without their experienced mentorship.

I would also like to thank **Mrs. Meeta Sharma(ARM), Mr. D Mohana Rao(ARM), Alternative Energy department, and Mr. Pali Rosha (Research Scholar), SEE** for their supervision and for providing me this learning experience. Many people, especially my fellow trainees and students from different colleges, have made valuable comment and suggestions on this proposal which gave me the inspiration to improve my assignment. At last, I want to thank all those people who directly or indirectly helped me for making this experience successful.

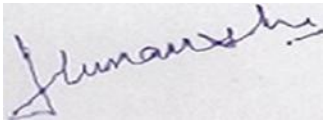

Himanshu Sharma

601601011

Abstract

Development of non-petroleum and clean energy sources for the transport industry is the main focus of recent developments in the fields of energy. Hydrogen being a renewable and clean fuel has the potential to be the energy carrier. Hydrogen can be produced by many sources either renewable or nonrenewable. The steam reforming reaction is extensively used in industries for hydrogen production. Dry reforming is one of the environmentally friendly processes for hydrogen production because it uses two major greenhouse gases for clean fuel production i.e. hydrogen. The catalyst deactivation due to coke deposition is one of the major difficulties with the dry reforming. Addition of steam in the reaction can significantly reduce the amount of coke deposition. H_2/CO ratio in the product gas is equals to 2 theoretically, which is very useful in its downward reactions. Ni-based catalysts are the most commonly used catalysts in the reforming reaction. Higher surface area and high dispersion of active metal are the most desired properties in reforming catalyst. In this project the effect of thermodynamic conditions (Temperature, Pressure and feed composition) on the conversion of reactant gases and yield of product gases is studied. The temperature range of 650-800℃, Pressure range of 5-20 bar, and S/C (steam-to-carbon) ratio of 0.50-2.50 are used in the study. Both CH_4 conversion and H_2 yield increase with an increase in temperature and amount of steam. Both CO_2 conversion and CO yield increase with an increase in temperature but decrease with increase in steam amount. High H_2/CO ratio can be produced at a lower temperature and decreases with temperature.

Table of Contents

List of Figures

List of Tables

Abbreviations

- **GHGs**- Greenhouse Gases
- **UNFCCC**- United Nations Framework Convention for Climate Change
- **CNG**- Compressed Natural Gas
- **SRM**- Steam Reforming of methane
- **POR**- Partial Oxidative Reforming
- **WGS**- Water Gas shift reaction
- **RWGS**- Reverse Water Gas Shift Reaction
- **ATR**- Auto Thermal Reforming
- **DRM**- Dry Reforming of Methane
- **TRM**- Tri-Reforming of Methane
- **SV**- Space Velocity
- **GHSV**- Gas Hourly Space Velocity
- **XRD**- X-Ray Diffraction
- **BET**- Brunauer-Emmett-Teller Analysis
- **TEM**-Transmission Electron Microscopy
- **SEM**- Scanning Electron Microscopy
- **EDX**-Energy-Dispersive X-ray
- **TGA**- Thermogravimetric Analysis
- **IOCL**- Indian Oil Corporation Limited
- **RKS-BM**- Redlich-Kwong-Soave with Boston-Mathias function
- **MFC**- Mass Flow Controller
- **NG**- Natural Gas
- **S/C Ratio**- Steam to Carbon ratio

CHAPTER 1
INTRODUCTION

1.1 Introduction

Growing industrialization and population explosion have put a huge pressure on the energy resources. Main sources in the current scenario are fossil fuels which are on the verge of ending due to rapid depletion and unorganized use. Combustion of fossil fuels causes emission of greenhouse gases (CO_2, NO_x etc.) which are causing environmental depletion (greenhouse effect). We have already started experiencing the results of climatic change like floods, droughts, and change in rain pattern.

The rapid depletion of fossil fuels and environment constraints has forced us to look for the cleaner alternative sources of energy. The cleaner sources of energy will help us to meet the emission standards and will help in protecting our environment. The main source of alternative energy is solar energy, wind energy, hydrogen energy, hydro energy etc.

The emission of greenhouse gases (GHG) results in enhancing the temperature of the earth atmosphere, this phenomenon is referred as greenhouse effect. The major GHGs are carbon dioxide (CO_2), methane (CH_4), oxides of nitrogen (NO_x), and CFCs etc. Their distribution (Figure 1) shows that the CO_2 and CH_4 are the two most important gases.

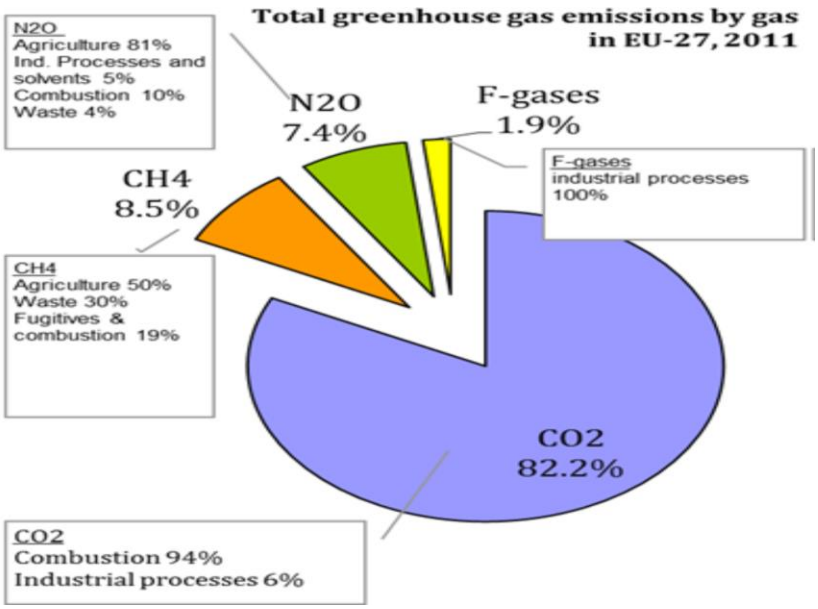

Figure 1 Greenhouse gas emission: (UNFCCC).

Hydrogen has been proposed as a clean fuel for transportation and stationary energy uses since its consumption releases only water vapor instead of greenhouse gases. Hydrogen can be used as a cleaner energy but hydrogen is not a source of energy but it is only a carrier of energy. Hydrogen must be produced from another primary energy source, be it renewable, like solar, wind, or biomass, or other non-renewable or fossil fuels such as coal or natural gas. CNG is used extensively in the transportation applications and mainly composed of methane, but methane itself is a greenhouse gas and can be used to produce hydrogen which is a clean fuel and can be used for our requirement. CO_2 is also a greenhouse gas which can be used for reforming of methane for production of hydrogen. So, reforming is a very useful process in which two major greenhouse gases are used to produce hydrogen which is a clean fuel.

Natural Gas	**Vol% (Dry basis)**
Methane	90.8298%
Ethane	4.95366%
Nitrogen	0.31118%
CO_2	2.405662
Propane	1.11873%
I-Butane	0.15031%
N-Butane	0.21288%
I-Pentane	0.01292%
M-Pentane	0.00482%
Relative Density	0.62

Table 1 Components of natural gas

1.2 Introduction to Hydrogen

Hydrogen is the most profuse element in the universe, burns clean and has the highest energy density per unit mass. However, hydrogen is not an energy source, only an energy carrier, and it is not generously available in nature and needs to be produced, either from water or other

compounds. If it is produced from water, it costs more energy to produce it than one would recover from burning it. Hydrogen can be produced from either conventional sources or from renewable sources. Conventional sources include Natural gas, methanol, naphtha, and renewable sources include biomass.

The fuel properties of hydrogen are-

- Complete combustion will give water, and nitrogen.
- High flame speed
- Low ignition energy
- A wide range of ignition limits
- Low density
- High diffusion speed

1.3 Hydrogen: Properties

PROPERTY	RANGE
Atomic number:	1
Atomic weight:	1.00782519
Formula:	H_2
Chemical structure:	H–H
Molecular weight:	2.0159
Appearance:	Colorless and odorless gas at room temperature
Density (gas):	0.08988 g L^{-1} (0°C, 1 atm.)
Density (liquid):	70.8 g L^{-1} (at -253 °C)
Melting Point:	-259.35 °C
Boiling Point:	-252.88 °C (at 1 atm.)
Solubility in water:	0.0214 cm^3 g^{-1} (0 °C, 1 atm.)
Energy content for 1 kg hydrogen (when reacting with oxygen to form water)	
Higher heating value:	141 900 kJ; 33 900 kcal; 39.4 kWh
Lower heating value:	120 000 kJ; 28 680 kcal; 32.9 kWh
Auto-ignition temperature:	500–571 °C
Explosive limits:	4–76% (vol. % in air)

Table 2 Properties of Hydrogen

1.4 Hydrogen: Compared with Other Fuels

Fuel	Net Energy Content(MJ/kg)(1)
Hydrogen	120.0
Methane	50.0
Natural gas	47.1
Diesel oil	42.6
Gasoline(Petrol)	43.4

Table 3 Energy content per unit mass

The hydrogen has the highest net energy content per unit mass as compared to the other available fuels. This property gives it a preference to the hydrogen over other fuels but the main problem is that the density of the hydrogen is lowest as compared to the other fuels. The hydrogen has the lowest energy density so to use to the hydrogen in transport applications a large volume of hydrogen will be required.

1.5 Hydrogen Production

The hydrogen and syngas(H_2/CO) are produced by various sources through a large variety of processes. Various liquid and gaseous hydrocarbons, like carbohydrates(2), alcohols, glycerol, biodiesel(3), and even solid feedstock like coal(4) or biomass are used for hydrogen production.

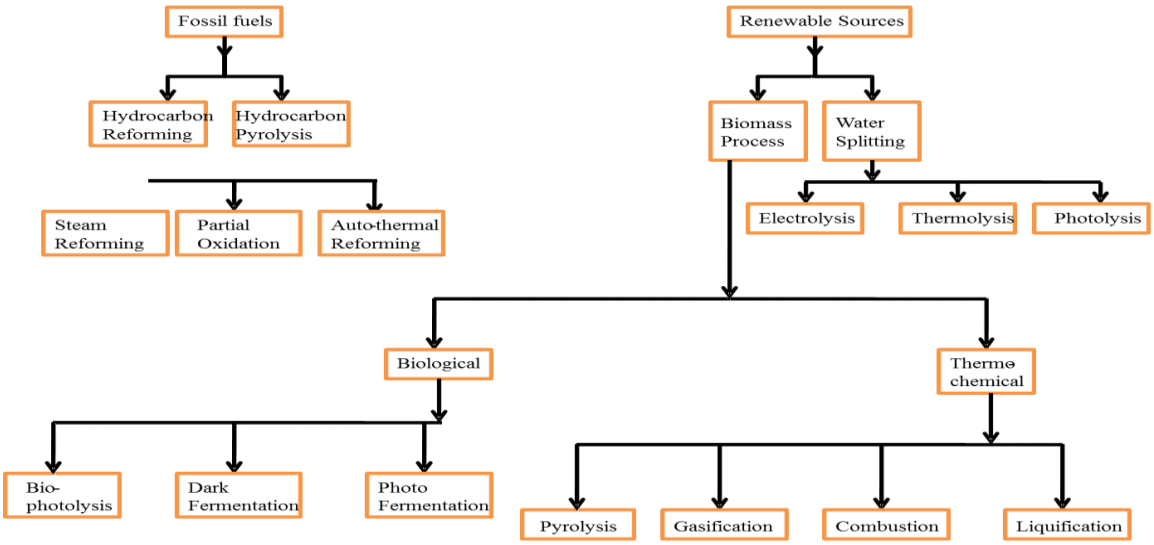

Figure 2 Hydrogen Production Techniques

1.5.1 Steam Reforming

Steam reforming is one of the most commonly used reforming reaction for industrial applications. The syngas produced from steam reforming has H_2/CO ratio in the rage of 2 to 4(2) depending upon the inlet feed conditions. The Steam methane reforming (SMR) is generally composed of two different reactions (i) the reforming reaction (Equation 1) and (ii) the Water Gas Shift reaction (Equation 2). The reforming reaction is endothermic in nature (206 kJ.mol^{-1}), and the WGS reaction is slightly exothermic (-41 kJ.mol^{-1}). Desulphurisation of the feed gas is an extra step in the reforming reactions to avoid catalyst poisoning. The amount of sulfur in the gas streams should be less than 1 ppmw (particle per million by weight)(2). Some important reactions that take place during the reforming with their enthalpies:

- Steam Reforming of Methane (SRM- Equation 1)

Equation 1 $CH_4 + H_2O \rightarrow CO + 3H_2$ $\Delta H_{298} = 205.9\ \mathbf{kJ.mol^{-1}}$

- Water Gas Shift Reaction (WGS - Equation 2)

Equation 2 $CO + H_2O \rightarrow CO_2 + H_2$ $\Delta H_{298} = -41\ \mathbf{kJ.mol^{-1}}$

- Boudouard reaction (Equation 3)

Equation 3 $2CO \rightarrow CO_2 + C$ ΔH_{298}= -172.4 kJ.mol^{-1}

- Coke gasification (Equation 4)

Equation 4 $C + H_2O \rightarrow CO + H_2$ $\Delta H_{298} = +131.3\ \mathbf{kJ.mol^{-1}}$

- Methane Cracking (Equation 5)

Equation 5 $CH_4 \rightarrow C + 2H_2$ $\Delta H_{298} = +74.6\ kJ.mol^{-1}$

- CO oxidation (Equation 6)

Equation 6 $CO + \frac{1}{2}O_2 \rightarrow CO_2$ $\Delta H_{298} = -283\ kJ.mol^{-1}$

1.5.2 Partial Oxidative Reforming

The partial oxidative reforming (POR) involves the reaction between natural gas and oxygen. It is an exothermic reforming. POR involves a heterogeneous catalyst and produces a syngas of H_2/CO ratio of 2. The temperature of 1000-1500°C and pressure of 1-80 bar is required for this reforming (5–7).

The partial oxidative reforming process possesses some thermodynamic advantages over the steam reforming:

A. POR is slightly exothermic in nature as compared to SR which is of endothermic in nature. So, the energy requirement in the POR will be less than steam reforming.

B. The syngas produced from this reforming has H_2/CO ratio of 2 and is useful for downstream utilization like in F-T processes.

C. The product gases of POR are extremely low in CO_2 content, so it would be easier to directly use the produced synthesis gas.

D. POR does not the use the expensive superheated steam.

1.5.3 Auto-thermal reforming (ATR)

ATR is an alternative and new technology which combines both the SRM and the POR. The resulting overall enthalpy of this reforming is closer to zero. A balance between both the reactions must be established, in order to achieve overall enthalpy close to zero. This reforming reaction is usually performed between the temperature range of 900-1500°C and in the high pressure range of 1-80 bar(2,5,7). The H_2/CO ratio of the syngas is almost close to 2 and depends on the feed composition (5,7).

1.5.4 Dry reforming

The Dry Reforming was first examined by Fischer and Tropsch over Ni and Co catalysts. DRM is an attractive environment-friendly process as it uses two major greenhouse gases (i.e. CH_4 & CO_2) and produces syngas which in turn can be used to produce clean energy(hydrogen). This is an endothermic reaction and requires a temperature range of 800℃-1200℃. The Dry reforming reaction usually occurs at atmospheric conditions. There are high possibilities of coke deposition on the surface of catalyst and deactivation during this reforming (8–11). Coke deposition mechanism depends on the reactant feed, type of active metal and support, interaction between support-active metal, and catalyst preparation method (12,13). The dry reforming reaction is mainly accompanied by 3 side reactions: (i) Reverse water gas shift reaction (Equation 2) (ii) Boudouard Reaction (Equation 3) (iii) Methane decomposition (Equation 5).

Equation 7 $CH_4 + CO_2 \leftrightarrow 2CO + 2H_2 \qquad \Delta H_{298K} = 247\ kJ.mol^{-1}$

The coke deposition in the dry reforming can be prevented either by (i) using catalysts that can suppress the rate of coke formation, or (ii) adding steam (14–17), or oxygen (15,18–20)to the inlet feed.

1.5.5 Tri-reforming

Tri-Reforming of Methane is a combination of Steam, dry, and partial oxidative reforming in a single reactor(21,22). The H_2/CO ratio can be easily controlled by varying the relative quantity of the reactants. The tri-reforming reaction is an energy efficient reaction as the O_2 supplied to the system results in *in-situ* heat generation which lowers the energy requirement of the system(Partial oxidation of methane, POM)(21). The produced syngas has H_2/CO ratio in the range of 1.5 − 2.0, and useful for the further downstream applications(18,21,23,24).

The problem with the TRM is that the presence of O2 can leads to the complete oxidation of the methane which is a highly exothermic reaction and release huge amount of energy, which can produce hot spots of the reactor section and temperature inhomogeneity in the catalyst bed.

Equation 8 $\mathbf{CH_4 + O_2 \rightarrow CO_2 + 2H_2O}$ $\mathbf{\Delta H = -880\ kJ/mol}$

So, in our study, we are not supplying oxygen in the system and only steam and CO_2 is supplied with the natural gas (Equation 9). In this reforming reaction, the molar ratio of H_2/CO can be easily varied by adjusting the feed composition of $CH_4/H_2O/CO_2$ (10,11). The addition of superheated steam to the feed composition gave us some advantage over the conventional dry reforming: (i) the coke deposition can be reduced by the oxidation of carbon species, and (ii) a wider range of H_2/CO ratio can be produced.

Equation 9 $\mathbf{2CH_4 + CO_2 + H_2O \rightarrow 5H_2 + 3CO}$

1.6 Use of Syngas

Syngas (Synthesis gas) is a very important gas, it is a mixture of mainly H_2 and CO. CO2 is also presents sometimes in trace amount. Syngas is a raw material for many important chemicals. The energy density of the syngas is 50% that of natural gas. It cannot be burnt directly but is used as a fuel source (26)

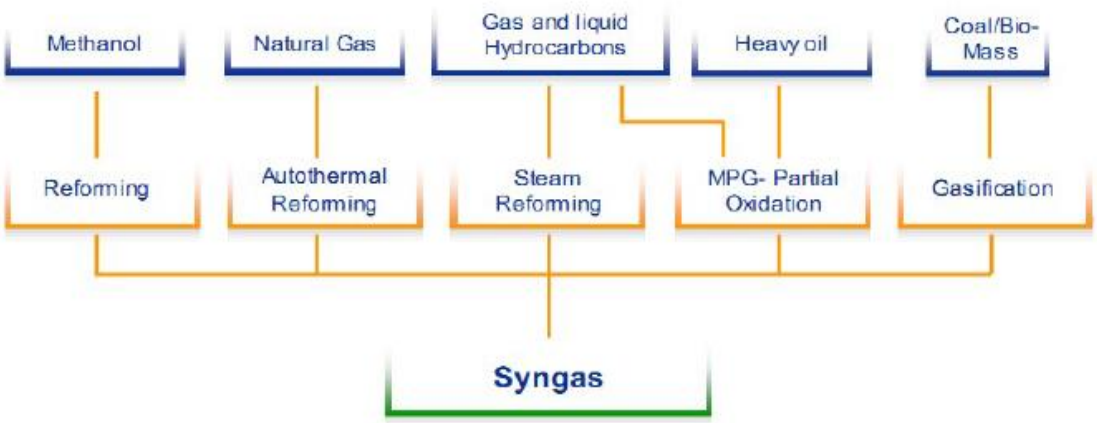

Figure 3 Syngas Production Methods(27)

Main benefits of the synthesis gas are(28)-

- For generation of alternative and renewable energy
- For waste to energy applications.
- For reduction of carbon emission
- Provide on-site power and hence reduces transmission losses

Syngas is used to make a large variety of fertilizers, fuels, solvent and synthetic materials(29).

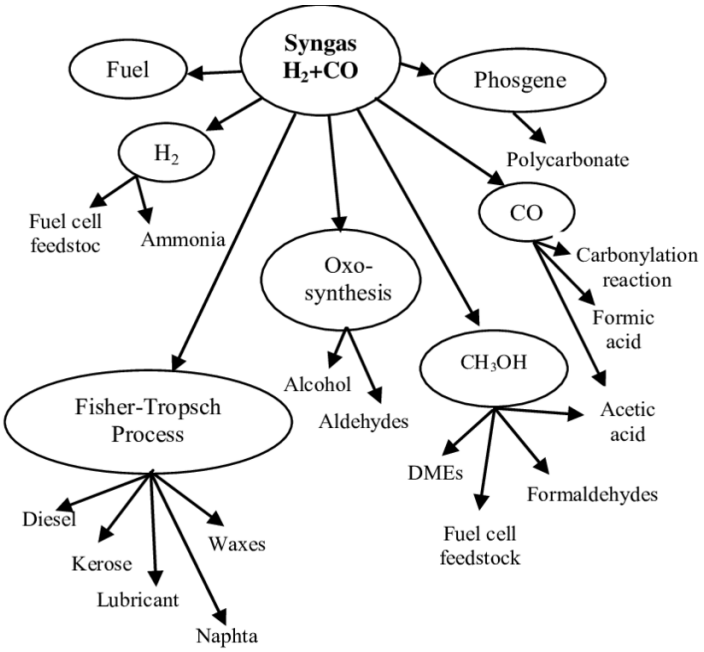

Figure 4 Use of Syngas in Chemical Industry (5,30)

CHAPTER 2
Literature Review

2.1 Catalyst, Catalyst activity, and Thermodynamic Conditions

The Ni-based catalyst is used extensively in the reforming reactions due to their high activity and stability during the reforming reactions. Ni metal is used mostly due to its lower cost and easy availability(31–35). The support material normally studied in the reforming reaction are Al2O3, MgO, MgAl2O4, ZrO2, SiO2, CeO2, TiO2, La2O3 etc. (36–40)

The main problem with Ni catalyst is the deactivation by the coke deposition and sintering (thermal degradation) of the metal particles due to the high temperature of the reactions. Many promoters are added with the Ni metal to prevent the coke deposition, improve support-metal interaction and thus enhancing the stability and the activity of the catalyst Promoters like Ba, Ca, K, Ce, Co, Sm, Zr, La, Mg etc are used due to their basic nature, which helps in improving the activity and stability of the catalyst(31,32,41–46).

Ni-catalyst promoted with Co and Ca are mostly used in reforming reactions due to lower cost and relatively higher availability. Zirconia (ZrO_2) is also studied in reforming reactions because of its some very useful properties which help in strong support-metal interaction and improvement in stability of the catalyst. The main properties of ZrO2 are its high ionic conductivity, high mechanical and thermal strength, fracture toughness, and oxygen ion mobility (47–51).

Itkulova *et al.* (52) studied the reforming reaction with Co-Pt metal catalyst supported on zirconia modified alumina The alumina support was modified with the varying amount of zirconia(5-10 mass%). The reforming reaction was performed in the temperature range of 300-755°C, P=0.1MPa, CO_2/CH_4=1/1. Th GHSV was kept 1000 h^{-1}. The main findings of the study were that addition of steam in the feed results in improvement of the process, the addition of promoter results in improvement in activity of the catalyst. The addition of ZrO2 to the support also improves the performance of the catalyst as it reduces the maximum temperature (by 40-50°C) required for complete conversion of the methane. The zirconia addition also improves the hydrogen production and H_2/CO ratio of the syngas produced. The conversion of reactant gases and yield of H_2 and CO always increase with an increase in the temperature.

Kim *et al.* (53) studied the performance of Ni/M-Al_2O_3 catalyst promoted with Sm, Ce and Mg oxides using the coke oven gas. The amount of Ni metal and promoter were kept 10 wt% and 5 wt% respectively. The catalysts were prepared by the wet impregnation method. The M-Al_2O_3 was treated with formic acid dissolved in methanol before the Ni impregnation to fill the pore spaces of the support. The reforming reactions were performed at T= 800 °C, P= 0.1 MPa. The effect of space velocity on the activity of the catalyst was studied by varying it from 36,000 to 72,000 L/(kg_{cat}·h). The methane and carbon dioxide conversions decrease with increase in the space velocity with every promoter. The Sm promoted catalyst showed the highest catalytic activity because Sm has higher electronegativity and basic properties which results in lower coke deposition, no sintering and a high degree of reduction of the active metal. The order of methane conversions for all space velocity ranges is; Ni/Sm-Al_2O_3>Ni/Al_2O_3>Ni/Ce-Al_2O_3>Ni/Mg-Al_2O_3. The extent of coke depositions was in the orders of Ni/Ce-Al_2O_3 >Ni/Mg-Al_2O_3 >Ni/Al_2O_3 > >Ni/Sm-Al_2O_3.

Sang *et al.* (54) studied the activity of Ni/α-Al_2O_3 catalyst promoted with MgO. The molar ratio of NiO-MgO was varied between 0-2. The catalysts were prepared by impregnation method. The reforming reactions were performed in the temperature range of 650-800^{o}C. The feed composition of $H_2O/CO_2/CH_4$ = 2.4/1.2/3 was used with a space velocity of 15530 L/g_{cat}h. The addition of MgO results in an increase in catalytic activity and stability. The addition of MgO into NiO/α-Al_2O_3 catalyst caused the formation of spinel phase $MgAl_2O_4$ and solid solution phase $MgNiO_2$ that led to improvements in catalyst activity and stability. The most suitable catalyst is (NiO-MgO) (2:1)/α-Al_2O_3 which showed high metal dispersion, and CH_4 & CO_2 conversion of 99.9% and 75.0% respectively.

Jang *et al.* (55) analyzed the thermodynamic equilibrium of reforming and side reactions using a catalyst(Ni–MgO–$Ce_{0.8}Zr_{0.2}O_2$). The study was done with of total Gibbs free energy minimization method. The reforming reactions were performed with a GHSV of 20000 h^{-1}. Their main interest was to study the effects of temperature (500-1000°C) and feed composition on the conversion, yield and coke formation. The CO_2/H_2O ratio was varied from 3:1 to 1:3, (CO_2 + H_2O)/CH_4 ratio was also varied from 0.9–2.90. It was concluded that the maximum temperature required for the maximum conversion of CH_4 and CO_2 depends upon the (CO_2 + H_2O)/CH_4 ratio. The conversion of CH_4 increase with an increase in temperature for all the

feed compositions. The negativeCO_2 conversion was observed for high CO_2/H_2O and (CO_2 + H_2O)/CH_4 ratio at a temperature below 550℃. The positive CO_2 conversion was occurred only at the high temperature due to the higher endothermic nature of dry reforming and stable nature of CO_2. The H2 yield increases with increase in (CO_2 + H_2O)/CH_4 ratio for temperature up to 750℃ but then decrease at higher temperature due to the reverse water gas shift reaction. The coke formation decreases with increase in temperature and oxidizing agents (CO_2+H_2O). The analysis showed that a (CO_2+H_2O)/ CH_4 ratio of at least 1.2 is required to avoid coke formation.

Lee *et al.* (56) examined the effect of the organic acid treatment on Ni/Al_2O_3 catalysts for the reforming reaction. The support was treated with the different organic acids such as formic acid, acetic acid, propionic acid, and oxalic acid. The reforming reactions were performed at a temperature of 750℃ and pressure 1.0 MPa. The feed composition $CH_4/CO_2/CO/H_2/H_2O$ = 1/0.38/0.29/2.09/1.2 was used with a space velocity of 36000 L/(kg_{cat}.h). The acid treatment improves the support-metal interaction and dispersion of active metal. The pKa value of acids alters the isoelectric point of the support surface which controls the dispersion of active metal. The catalyst pretreated with formic acid the smallest particle sizes of active metal and the highest catalytic activity.

Olah *et al.* (57) studied the catalyst NiO/MgO in the bireforming of natural gas. The reforming reactions were performed in the temperature range of 800-950 and pressure range 5-30 atm. The results showed that the conversion of CH_4 and CO_2 increase with an increase in the temperature but decrease with increase in the pressure. the conversion of CH_4 also decreased with increase in the GHSV. It was also concluded that the conversion of CH_4 and CO_2 remain constant over an extended period of time in the temperature range used. The H_2/CO ratio of the syngas produced can also be easily controlled by changing the relative quantity of CO_2 and steam in the feed.

Son *et al.* (58) studied the activity of $Ni/\gamma\text{-}Al_2O_3$ catalyst stabilized by a steam pretreatment at 850°C. The steam treatment helped in the removal of the unstable alumina to prevent the coke deposition on the catalyst surface during the reaction. The reforming reactions were performed the feed composition $CH_4/CO_2/H_2O//N_2$ = 1:0.4:0.8:1.6 with GHSV of 50.666 l/g/h. The results showed that steam-treated $Ni/\gamma\text{-}Al_2O_3$ catalyst gave the thermodynamically possible highest conversion (98.3% for CH_4 and 82.4% for CO_2) and the H_2/CO ratio of 2.01.

The coke deposition on the steam-treated catalyst was 3.6% and 15.4% on conventional catalysts. The carbon resistance was increased significantly after the steam treatment and it improves the activity and the long-term stability.

Koo et al. (59) examined the effect of Ce (6 wt%)-promotion on the performance and activity of (12 wt%)Ni/Al_2O_3 catalysts. The effect of loading sequence of Ni–Ce was also studied. The reforming reaction was analyzed with the feed composition of CH_4:H_2O:CO_2:N_2 = 1.0:0.8:0.4:1.0 with an SV of 530,000 ml/g_{cat}.h in the temperature range of 650°C to 750°C. The co-impregnation of metals gave the better metal dispersion and had higher oxygen storage capacity than the sequential impregnation and hence the activity of the co-impregnated catalyst was better than the sequential impregnated catalysts. The catalytic activity was increased due to the intimate contact between Ni and CeO_2 on the surface of the catalyst and that the interaction between Ni and CeO_2 depends strongly on the Ni–Ce loading procedure during the catalyst preparation.

Soria *et al.* (11) analyzed the effect of the amount of steam added(1%, 2%, 5% vol) on the activity and product distribution using a Ru/ZrO2-La2O3 catalyst. The thermodynamic analysis of the reforming reaction was done using the Gibbs free energy minimization method. The total flow rate of gases was kept 100 mL/min. The observations showed that the conversion of CH_4 increases whereas the conversion of the CO_2 decreases with increase in the amount of steam. The negative CO_2 conversion was also observed below 450℃ for a high amount of steam content. The H_2O conversion highly dependent of the temperature of the reforming, below 550℃ the conversion increased with increase in temperature due to the occurrence of steam reforming but at a higher temperature, the conversion was reduced due to the occurrence of RWGS reaction. The steady increase in H_2 yield and decrease in CO yield was observed with increase in the steam content. It was also observed that H_2/CO ratio was also dependent on the amount of the steam added. The addition of steam also improved the stability of the catalyst.

Baek *et al.* (61) study the effect of CeO_2 promotion on $Ni/MgAl_2O_4$. The catalyst was prepared by the co-impregnation method. The reforming reaction was tested at a temperature of 850°C and Pressure of 1.0 MPa. The feed ratio (CH_4/CO_2/H_2O/N_2) of reactant was kept 3/1.2/3/3 with different SV of 5,000 and 200,000 mL/g_{cat}/h. The result of the study showed that the promoted

catalyst has high catalytic activity and stability as compared to unpromoted catalysts. The addition of promotion enhances the support-metal interaction and strong support-metal interaction results in better dispersion of nickel metal. The mobile oxygen in the promoter also prevents the particle agglomeration. The promoted catalyst also has high resistance to coke formation due to strong support-metal interaction

Özkara-Aydınoğlu (10) analyzed the thermodynamics of the reforming using Gibbs free energy minimization method. The study was focused on understanding the effects of process variables such as temperature, pressure, and inlet feed conditions $CH_4/H_2O/CO_2$ ratios on product yields and the conversion of reactants. The reforming reactions were performed in the temperature range of 200-1200℃, steam to carbon ratio of 0-0.50, and pressure of 1 and 20 bar. The results of the study showed that the addition of extra steam increased the CH_4 conversion and 100% conversion was obtained at a temperature above 800℃. The increase in the steam resulted in a decreased CO_2 conversion. The rate of H_2O conversion was also decreased at high temperature due to the occurrence of dry reforming and reverse water gas shift reaction. The H_2 yield increases rapidly at low temperature but dampens at high temperature because of dry reforming and RWGS reaction. The study showed that reforming is a complex network of various reaction which occurs at different temperature regions and with different feed compositions. The increase in pressure was not favorable for the reforming reactions as it lowers the conversion of reactants and yield of products.

Koo *et al.* (62) studied Nano-sized Ni catalyst in the reforming reaction. The active metal was support on the Mg-Al mixed oxide support. The ratio of Mg/Al was varied to study its impact on the coke formation. The reforming reactions were carried out in a temperature range of 650°C to 750℃ for 15h at atmospheric pressure. The feed composition of CH_4: H2O: CO2: N_2 = 1:0.8:0.4:1 with GHSV of 530,000 ml/ ($h.g_{cat}$) was used in the reforming. The highest CO2 conversion was observed at Mg/Al ratio of 3.5 whereas the highest CH4 conversion was obtained at Mg/Al ratio of 0.50. So, it was concluded that increase in Mg/Al ratio results in better CO_2 adsorption and increase in CO_2 conversion. The catalyst with Mg/Al ratio of 0.50 had the highest catalytic activity and coke resistance because of nano-sized nickel particles.

Koo *et al.* (63) also studied the effect of promotion of MgO on the activity of the Ni/Al_2O_3 catalyst in the reforming reactions. The catalysts were prepared by the incipient wetness

method. The reforming reactions conditions were kept as same that was used in previous case(62). The results concluded that catalyst promoted with 20 wt% MgO has the highest catalytic activity and high coke resistance. The addition of MgO promotes the formation of $MgAl_2O_4$ spinel phase. $MgAl_2O_4$ is stable at high temperature and promotes the strong support-metal interaction.

2.2 Summary of Literature review

The literature showed that the Ni catalysts are extensively studied for the reforming reactions. The addition of steam in the feed has several impacts on the yield products and conversion of reactants. The temperature has an important role in the reforming reaction, it was concluded that conversion of CH_4 and CO_2 increases with increase in the temperature. The H_2 yield is also dependent on the temperature and steam content in the feed, as at low temperature and high steam content H_2 yield is high but the rate in increase reduces at high temperature even with high steam content. The increase in the pressure is not favorable for the reforming reaction as it reduced both conversions of reactant and yield of products.

2.3 Objectives of the study

The main objectives of our study on the basis of the literature available is "the study of effect of thermodynamic conditions (temperature, pressure, and feed composition) on the conversion of reactants and yields of products." The effect of high pressure conditions and conversion of steam in the reforming reactions are not described properly in the available literature. The syngas produced by reforming reaction at high pressure will be useful for the downstream application e.g. in the F-T synthesis.

The temperature is varied from 650℃ to 800℃, pressure is varied from 5bar to 20bar, and steam to carbon ratio is varied from 0.50 to 2.50.

CHAPTER 3
CATALYST AND CHARACTERIZATION TECHNIQUES

3.1 Catalyst

Catalysts are the chemical compounds that alter the rate of reaction. It offers an alternative path for the reaction with lower activation energy. The catalysis reactions are of two types (a) heterogeneous and (b) homogeneous catalysis. Heterogeneous catalysis is mainly involved in reforming reactions because the inlet reactants are generally in gaseous or liquid state and the catalyst is in solid form. The catalyst can never change the equilibrium. Heterogeneous catalysis processes (Figure 5) involves the absorption of the reactants on the surface of the catalyst where the products are formed; in the end, the catalyst is "regenerated" to its initial state by desorption of the products(7).

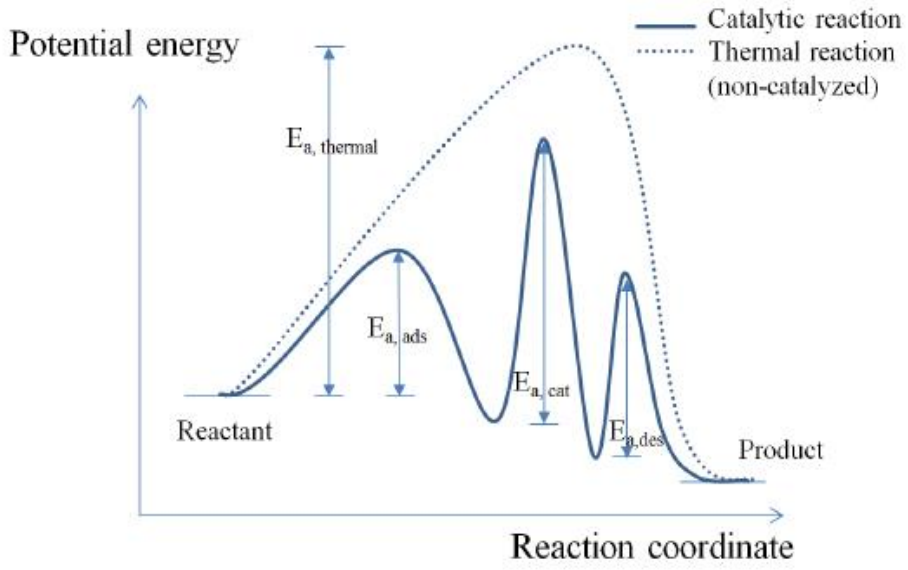

Figure 5 Effect of catalyst on the reactions

A solid catalyst consists of mainly three parts(64–67)-

1. Catalytic agent/ Active Metals
2. Support/Carrier
3. Promoters and inhibitors.

Catalyst agents are the active sites in the catalyst. The activity of any catalyst depends upon the availability of these active sites. Active phases (metals, metal oxides, and metal sulfides) should be well dispersed on the surface or in the pores of supports as nanoparticles. Catalyst

supports (carriers) are porous materials having high surface area and have significant pore volume and capacity for providing stable, and well-dispersed catalyst. Degree of dispersion of the active metal on the surface of support tells us about the availability of active sites. Supports provide the physical form, and mechanical resistance to the catalyst. Promoters added during preparation of catalyst and improves the activity/selectivity/stability of the catalyst. Promoters are of two types (i)physical (ii)chemical promoter depending on the manner they improve the catalyst performance. Catalyst stability depends on the poisoning and sintering of the active phases. The poisoning is referred as either permanent or reversible adsorption of foreign species at the active sites whereas the sintering is the reduction in surface area due to accumulation of active phases at elevated temperatures.

Industrial catalysts are of various shapes eg. spheres, rings, pelletes, and tablets(Figure 6). The synthesis of catalyst involves various stepes and the conditions at each step influence the properties/characterstics of the catalysts. So, great care must be taken during the synthesis for the desired properties of the catalyst.(68–70).

Figure 6 Shapes of catalysts (BASF, Ludwigshafen, Germany).

Following steps are involved in a general catalytic reaction over a porous catalyst (Figure 7)(68)

1. The diffusion of reactant into the boundary layer of the catalyst surface.
2. Diffusion of the reactants into the pores.
3. Adsorption of the reactants on the inner pore surface
4. The occurrence of a chemical reaction
5. Desorption of the products
6. Diffusion of the products from the pores
7. Diffusion of the products to the gas phase

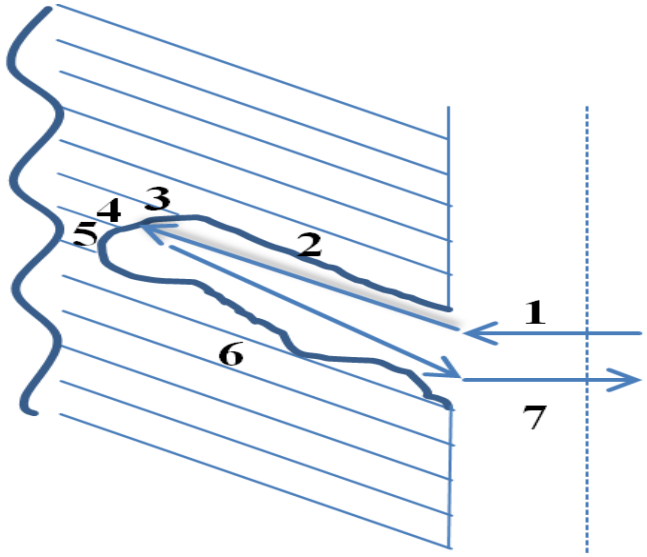

Figure 7 Mechanism of catalysis (taken from (68))

3.2 Deactivation of Catalyst

The catalysts are designed for high activity, but they lose their activity over a period of time due to different phenomena. Understanding these catalyst deactivation phenomena is important. The deactivation phenomena(37,71–75) can be classified into several types such as poisoning, catalyst fouling, thermal degradation and sintering, volatilization of active components. Deactivation can influence conversions of reactants and/or selectivity of the reactions (71–74,76).

3.2.1 Coking of Catalysts

The activity of catalyst is proportional to the active surface area of the catalyst as it provides the surface for the reactions to occur. Fouling is defined as the physical

deposition of the components on the catalyst surface or in the pore spaces(77). Catalyst fouling results in the decrease of the required specific surface for reaction to occur and for a high catalyst activity. The carbon produced in the reforming reaction blocks the pores of the catalyst and reduce the area of the active site for the reforming reaction. Carbon deposits are likely to be produced in the reforming reactions. The rate of deactivation of the catalyst depends on the conditions during the reaction such as feed gas composition and temperature. Basically, extant of coking depends upon the rate of coke generation and rate of its gasification. To avoid the coking the catalyst supports are chosen in such a way that it enhances the rate of gasification. Coking results from a "too low" gasification rate as compared with the rate of carbon-deposition. Rostrup-Nielsen et al. (78) have explained various methods for enhancing the catalyst activity with respect to coking:

- Enhancement in the adsorption of steam or CO_2(79).
- decrease the activation rate of hydrocarbons(2,79)

3.2.2 Sintering and thermal degradation of catalysts

Reforming reactions are favorable at high temperatures for higher activity, but high temperatures can cause the thermal deactivation of catalyst(80). Sintering is a type of thermal deactivation. Sintering effects are generally irreversible. It reduces the specific surface area, active metal surface area, and/or pore volume(39).

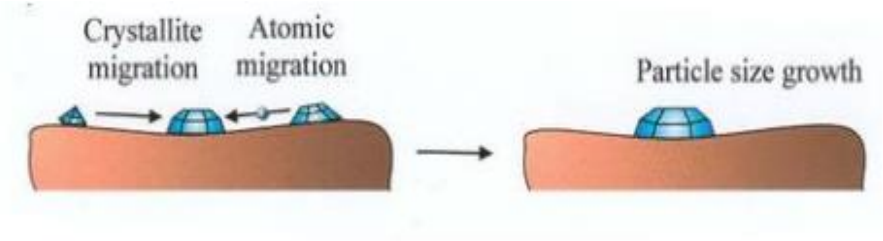

Figure 8 Deactivation by Sintering

Volatilization of active metals and phase transformation is also a reason of deactivation and loss of activity(5,37,68,72,81,82).

3.2.3 Catalyst poisoning

Catalyst poisoning is a chemical phenomenon of deactivation. Poisoning occurs due to strong chemisorption and strong interactions between active metals and third

compounds (37,83)). The presence of sulfur in the feed gases is the main reason of poisoning in the reforming reactions because sulfur will react with Ni and forms Ni-sulfide which is stable in nature (7). A desulphurization reactor is always installed before the action reactor to remove the sulfur content form the feed gases.

3.3 Promoters for catalytic performance

Promoters are used to improve the activity, the selectivity, and the stability of the catalyst. Promotion in the reforming catalyst is used to reduce coking possibilities. Bimetallic catalysts are also of special interest because in this process two different metals are combined to enhance the properties of catalyst i.e. stability, selectivity, and performance. The synthesis of the bimetallic catalyst is similar to the concept of alloying. The main types of bimetallic catalyst used in the reforming reaction are-

- Catalyst with two different noble metals like Pt-Pd. These can only be used for some special application because of their higher cost.
- Catalyst made by alloying a non-noble with a noble metal. These catalysts are widely studied for reforming reactions. Ni-Pt is the most reported catalyst in this category.
- By alloying two different non-noble metal with each other. They are the most attractive due to their lower cost. Ni-Co is the most studied catalyst in this category for the reforming reactions.

3.4 Synthesis of heterogeneous catalysts

Catalysts play a very important role in a chemical process, they are the most important aspect of any chemical reactions. The design and preparation of the catalyst are a very important step as it decides the properties of a catalyst. Special care must be taken during the preparation of the catalyst. There are some very useful requirements of the catalyst which must be fulfilled-

1. Low cost of the raw material and preparation method
2. Easy reproducibility of the catalytic properties
3. Low deactivation rate
4. High selectivity towards the desired products

5. High mechanical and thermal strength.

There are lots of methods available for the catalyst synthesis e.g. Impregnation, precipitation, and Sol-gel etc. The precipitation and impregnation methods are most commonly used method for the industrial applications.

In impregnation method, a metal(s) solution is impregnated upon the surface of the support. The selected support material should have a high specific surface area. This method is the simplest method among all the preparation methods. Special care of stirring rate, time and calcination temperature is required for the proper synthesis of the catalyst. The problem with this method is that only small fraction of metals can be doped on the support. The catalyst synthesized by this method is also known as supported catalysts.

In the precipitation method, a precipitator is added in the solution and the solution is left till the precipitation occurs. The catalyst synthesized by this method is known as a bulk catalyst as the composition of the whole catalyst could be same. Special care of pH, stirring conditions, drying temperature, calcination temperature and time should be taken for proper catalyst preparation.

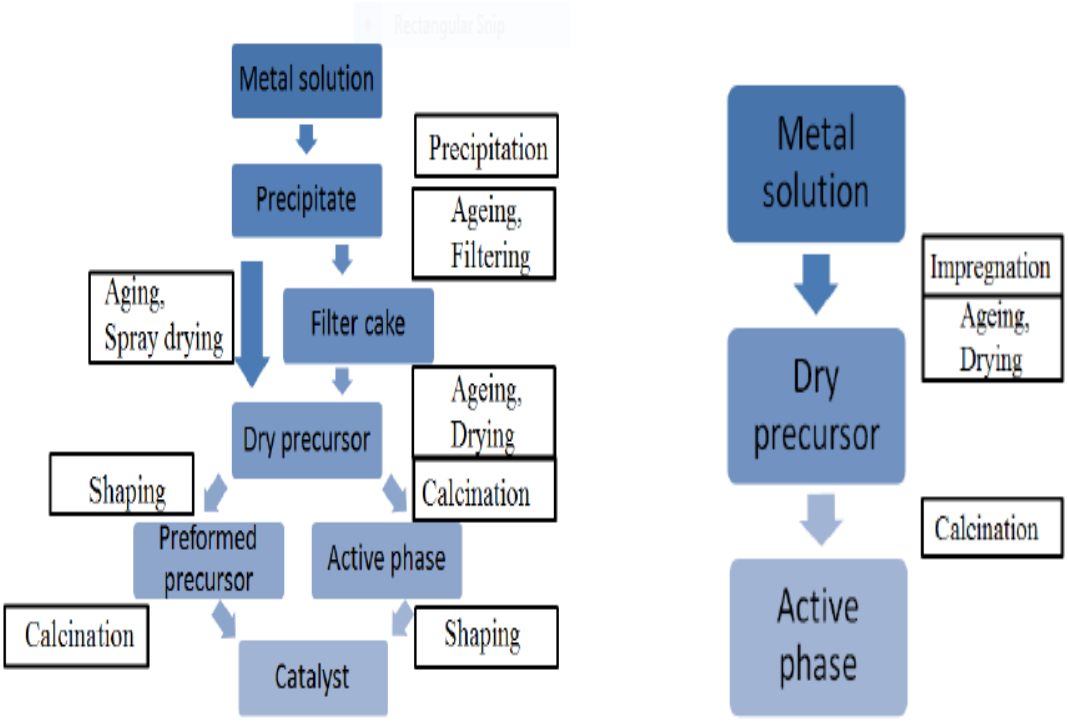

Figure 9 Different catalyst preparation methods(7)

3.5 Characterization of Catalysts

Catalyst characterization is helpful in understanding the physical and chemical properties of the catalyst. The better understanding of the catalyst properties is very helpful in predicting the behavior of the catalyst towards a reaction. The activity of the catalyst is directly linked to the properties of the catalyst. The influence of preparation parameters on the catalyst and the deactivation methods are also studied by the characterization techniques(84). The commonly used characterization techniques are as-

3.5.1 X-Ray Diffractometry (XRD)

XRD or XRPD (X-Ray Powder Diffractometry) is a very useful analytical method for characterizing the crystalline materials. It is a non-destructive method and used for identification of phases, crystal structure, and unit cell size. XRD also measures the average spacing between the atoms and orientation of the grains. XRD is based on the constructive interference between the monochromatic X-ray and crystal sample(85). The calculation is done on the basis of the examination of intensity of a X-ray beam scattered by the sample as a function of the striking and scattered angle(73,75). The basic function of diffractometry is to check diffracted X-ray from the material and to store its intensity as a function of diffractor angle(86). The constructive interference between two parallel planes of atoms will happen when the Bragg's law (Equation 10) will be satisfied. The diffraction pattern for every phase is unique even their chemical composition is same. This uniqueness in the diffraction pattern of each phase helps in finding the presence of characteristic crystalline phases (87,88).

Equation 10 $$2\,d\sin\theta = n\lambda$$

Here, θ is the X-ray incident angle, d is the spacing between the two diffraction planes, n is an integer, and λ is the wavelength of the X-ray.

Identification of the phase is done by comparing the diffraction pattern of the sample with the reference phase or with a database. A database such as Powder Diffraction File (PDF) distributed by the International Centre for Diffraction Data contains a list of several crystalline phases (ICDD)(73,74)

Figure 10 Powder XRD apparatus

The crystal particle size in the sample can also be estimated from this analysis with the Scherrer equation (Equation 11). According to the Scherrer equation (73,89)by:

Equation 11 $$L_{hkl} = \frac{k_{scherre}\lambda}{\beta cos\theta_o}$$

Where L_{hkl} is the crystallite thickness in direction perpendicular to the diffraction plane (hkl), λ is the wavelength, θ_0 is the half diffraction angle/Bragg angle, β is the breadth of diffraction profile (Full width at half maxima).

3.5.2 Specific Surface area, pore size, and Pore Volume Determination

This analysis is helpful in understanding the extent of dispersion of active metal on the catalyst Higher specific surface area catalyst are always desirable as they provide a higher degree of active metal dispersion. The specific surface area of a catalyst is calculated through physical adsorption of a gas on its surface and by measuring the amount of adsorbed gas corresponding to a monomolecular layer on the surface(90,91).

The pores are formed during the calcination of the catalyst. The pore size determines the internal surface area and availability of the active sites to the reactants. The pores are divided into three groups- micropores (size less than 2 nm), mesopores (between 2 nm to 25 nm) and macropores (larger than 25 nm). The pore size distribution is determined by the mercury porosimetry(92,93). The geometry of pores is examined by the adsorption of gases at low pressure e.g. N_2-physisorption(94).

3.5.3 Electron Microscopy

The electron microscope is a microscope which use an electron beam to create an enlarged image of an object. The electron microscope used a large number of lenses and low wavelength electrons to form an enlarged image of the object(71,72). The electron microscopy technique is helpful in understanding the morphology and structure of the catalyst. There is two types of electron microscopy (a)Transmission electron microscopy (b) Scanning electron microscopy.

TEM is an electron microscopy in which an electron beam passing through a very thin specimen interacts with the specimen(68,71,73,95). Scanning Electron Microscopy (SEM) scans a sample with focused electron beam and generate its image. In TEM analysis the sample are very thin because transmission phenomenon is used for generating image whereas thin sample are not required in the SEM analysis(96). Energy-dispersive X-ray spectroscopy coupled with SEM is used for identification and to quantify the elements. EDX technique is based on the X-ray fluorescence. The SEM instrument used in this study is a JEOL, (JSM-6610 LV Model) from JAPAN.

Resolution:	HV Mode (3.0 nm, Acc V 30 kV, WD 8 mm, SEI), LV Mode (4.0 nm, Acc V 30 kV, WD 5 mm, BEI)
Magnification:	5X – 3, 00,000X
Probe Current:	1pA - 1 µA
Vacuum Pressure:	10 - 270 Pa
Accelerating Voltage:	0.3 – 30 kV
The coating material:	commonly carbon, Ag, Au, Pt or alloy.
For organic materials	
Fixation:	To preserve the structure
Drying:	Moisture must be removed
Coating:	To conductive the sample
For Inorganic materials	
For metals:	No need for preparation
For non-metallics:	Need to be coated

3.5.4 Thermogravimetric Analysis (TGA)

Thermogravimetric analysis or thermal gravimetric analysis (TGA) is a thermal method of analysis in which the change in mass of a catalyst is measured with respect to increasing temperature under specific gas environment and heating rate. TGA is used to determine the thermal stability, moisture content and volatile materials. This technique is helpful in determining the reaction kinetics of catalysts with reactive gases(97). Thermogravimetric analysis (TGA) is performed on thermogravimetric analyzer. It continuously measures the change in mass of the catalyst with the temperature over a period of time. Heating rate, amount of catalyst, and nature and flow of carrier gas are the main parameters affecting the TGA. The plot of remaining mass on y axis versus either temperature or time on x-axis is drawn with the help of collected data. This plot is knownn as TGA curve of the material. The different decomposition patterns of the materials are helpful in identifying the material through TGA analysis.

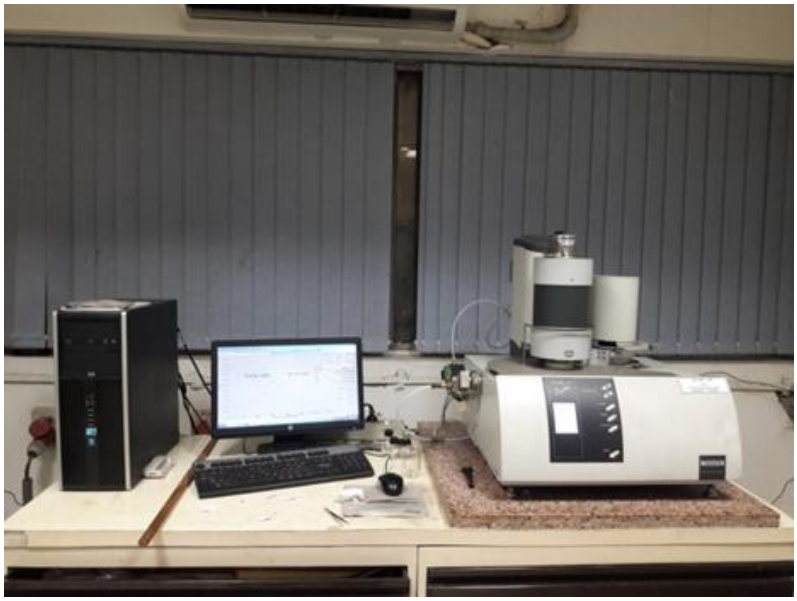

Figure 11 Thermo-Gravimetric Analyzer

3.6 Commercial Catalyst

The commercial catalyst used in the reforming reaction mainly consists of Nickel and Calcium metal on an alumina support. The catalyst pallets are of cylindrical shape and holes are present on the catalyst to provide spaces for the reaction. The activation of the catalyst was done by the standard activation method followed by the IOCL R&D center.

CHAPTER 4
Simulation Studies

4.1 Simulation Studies

The following steps are used for the simulation study-

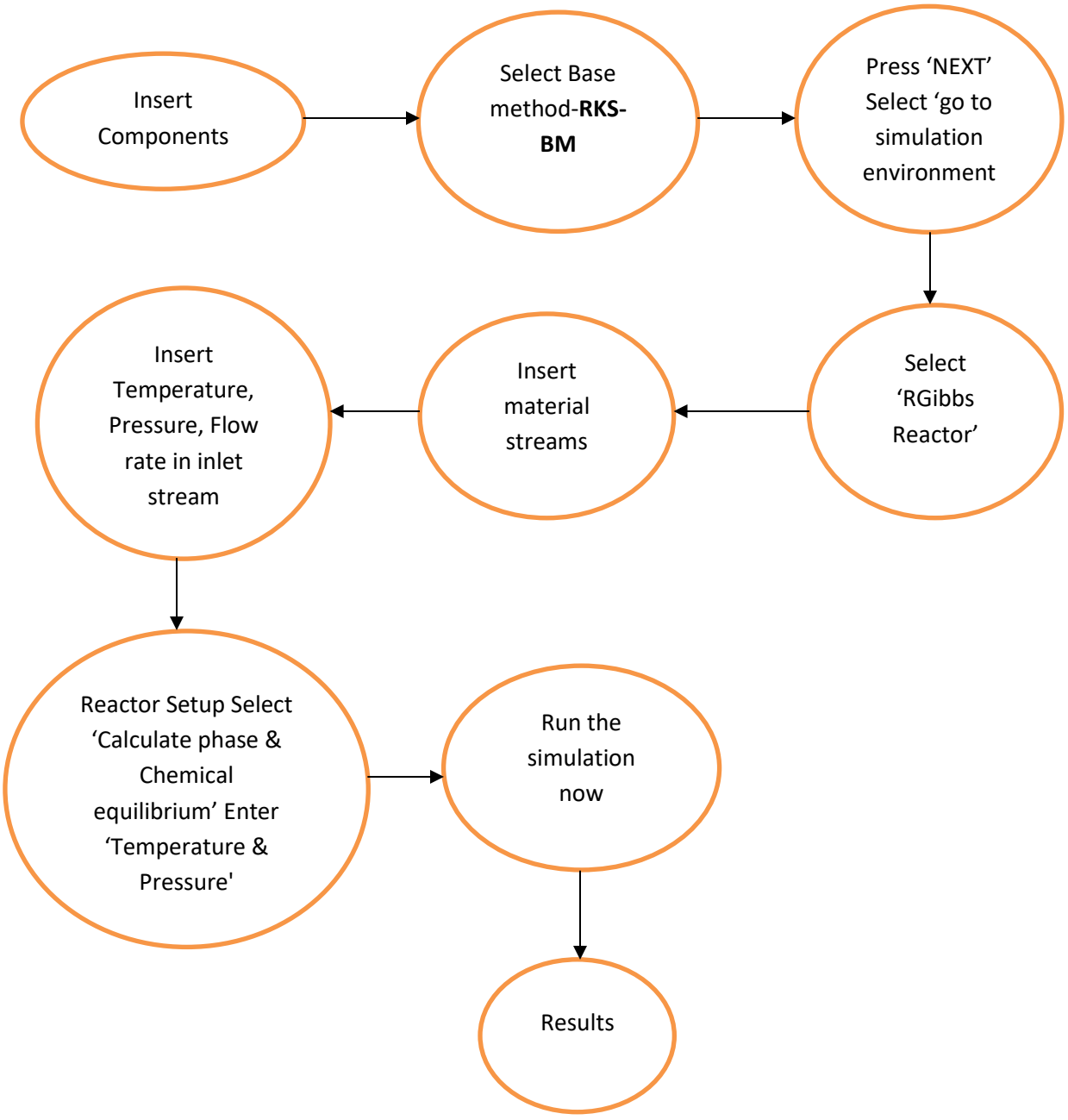

Figure 12 Flow chart of the simulation

The simulation study of the reforming reaction is done with the help of “Aspen Plus” software. The sensitivity analysis of the reaction is also done to examine the effect of temperature, pressure and steam content on the conversion of reactant and yield of products. In Figure 13 the steps in carrying out the sensitivity analysis are shown.

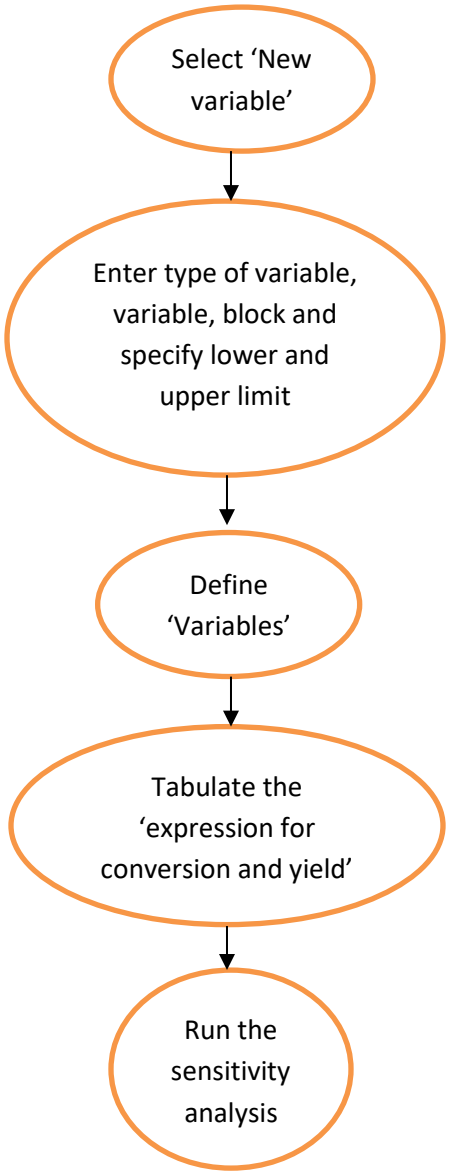

Figure 13 Sensitivity analysis flow chart

4.2 Result of simulation study

4.2.1 Effect of Temperature & Steam content

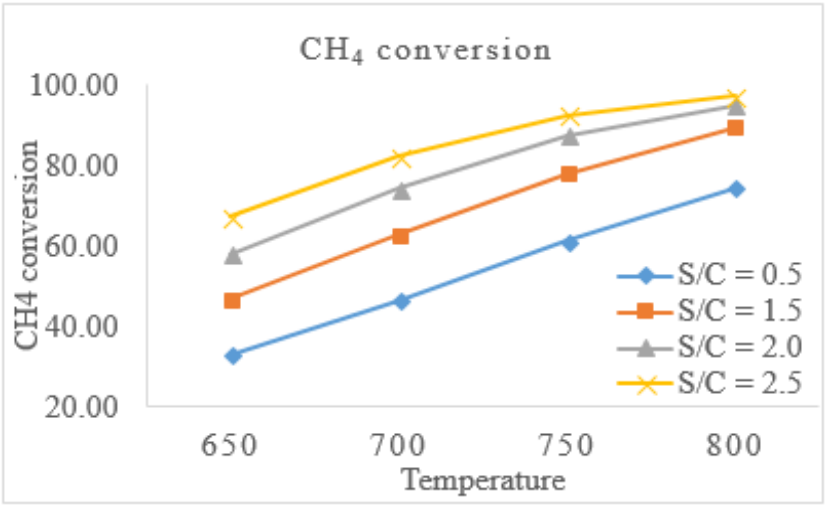

Figure 14 CH_4 conversion(Simulation)

In Figure 14 the effect of temperature and steam content is shown, the CH_4 conversion increases with increase in both temperature and steam content. At high temperature and high steam content, maximum CH_4 conversion is shown because methane becomes a limiting reagent and consumed in both steam and dry reforming(10,11,98,99).

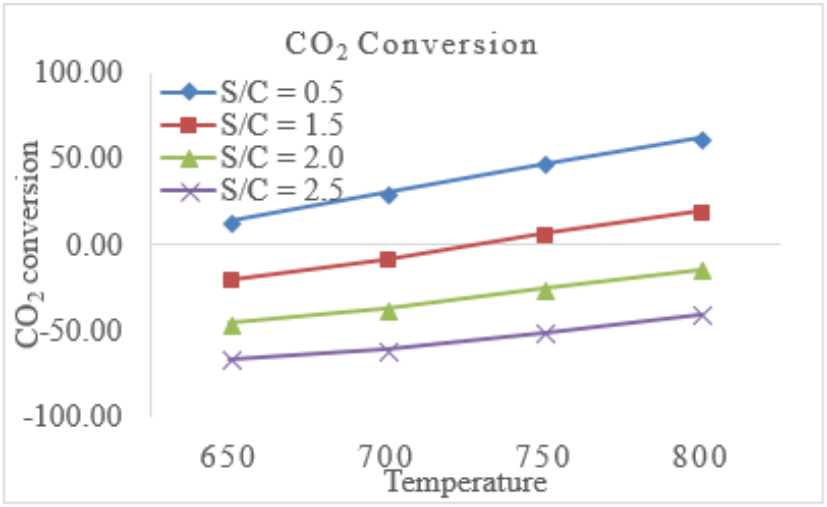

Figure 15 CO_2 conversion(Simulation)

In Figure 15 the effect of temperature and steam on CO_2 conversion is shown and this shows that addition of steam caused a decrease in CO_2 conversion. The CH_4 react more with H_2O as compared to the CO_2 because of the more stable nature of the CO_2(13). The

negative trend at low temperature and high steam content shows that water gas shift reaction is more dominant and suppress the dry reforming reaction and results in the production of CO_2.

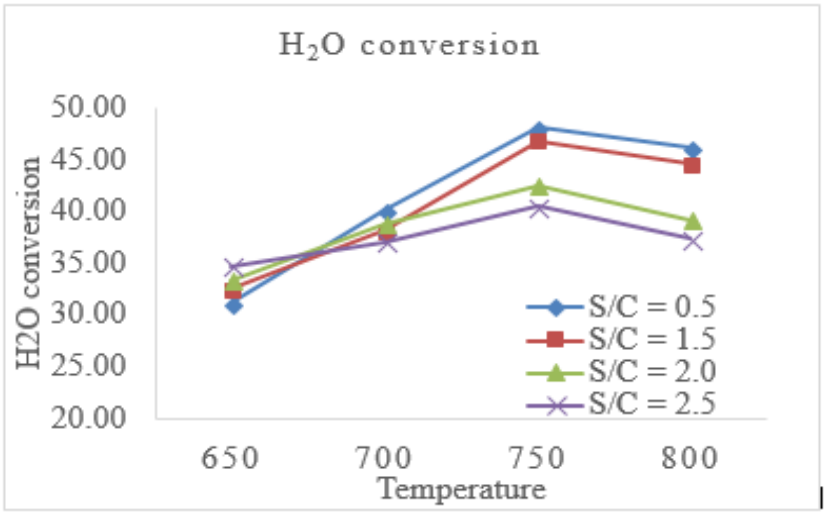

Figure 16 H_2O Conversion(Simulation)

Water conversion is shown in Figure 16 and it is shown that the conversion of H_2O doesn't increase with an increase in steam content due to the fixed amount of CH_4 and CO_2(13). At lower temperature the H_2O conversion increase with steam content because of the higher contribution of both steam reforming and WGS. The rate of H_2O conversion dampened at high temperature due to RWGS and Dry reforming, as they are dominant at high temperature. Although the steam reforming will be dominant with the increase in steam content but at high temperature, the dry reforming becomes more important and will affect the conversions(6,10,11,100).

The yield of both products is shown in Figure 17 and Figure 18. The H_2 yield increase sharply with increase in steam content at a lower temperature due to the combined effect of steam-dry reforming and WGS reaction. At high temperature, the H_2 yield not increase with an increase in steam content may be because of the occurrence of dry reforming and RWGS reaction, as dry reforming yields less hydrogen and RWGS consumes hydrogen. The CO yield decrease with increase in steam content at a lower temperature due to the WGS reaction which consumes the CO and reduces its yield. At the higher temperature, high CO yield is obtained because of the RWGS reaction which produces more CO.

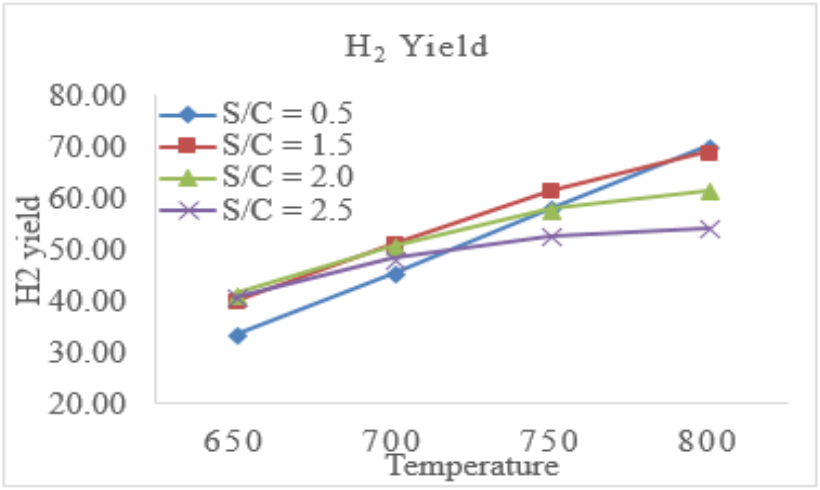

Figure 17 H_2 Yield(Simulation)

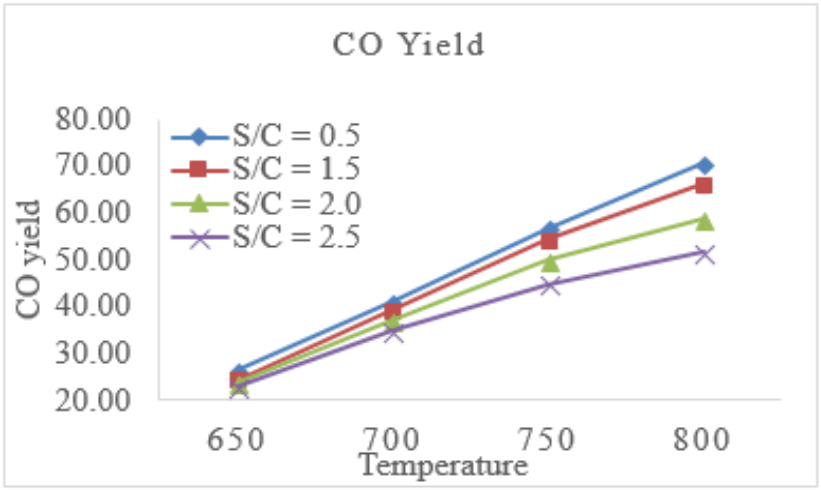

Figure 18 CO Yield (Simulation)

High H_2/CO ratio is produced at a lower temperature due to the WGS reaction and steam reforming which produces a higher amount of hydrogen. The addition of steam increase results in an increase in H_2/CO ratio because it enhances the steam reforming which yields more hydrogen. At higher temperature low H_2/CO ratio are produced due to the occurrence of RWGS reaction which decreases the H_2 yield and increases the CO yield.

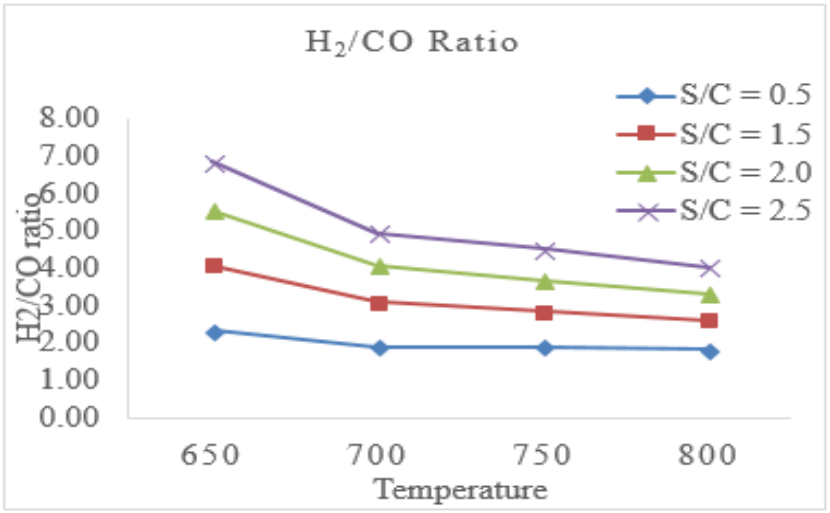

Figure 19 H_2/CO Ratio (Simulation)

The combined steam-dry reforming is dominated by different reaction with respect to different temperature and steam content. The reforming is a complex multi-reaction system(10,11,99,101).

4.2.2 Effect of Pressure & Steam content

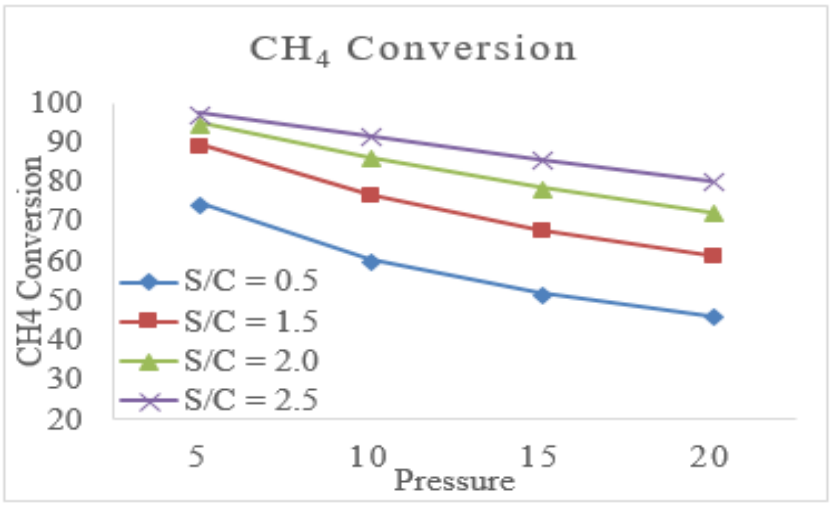

Figure 20 CH_4 Conversion with Pressure(Simulation)

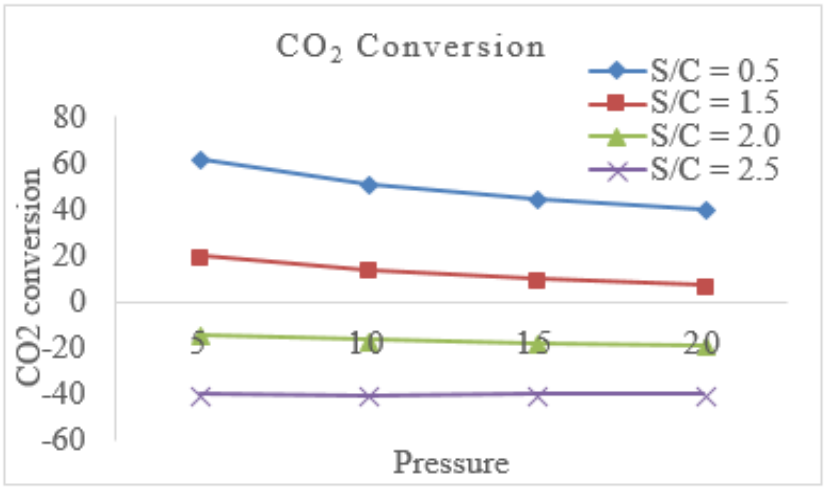

Figure 21 CO_2 Conversion with Pressure(Simulation)

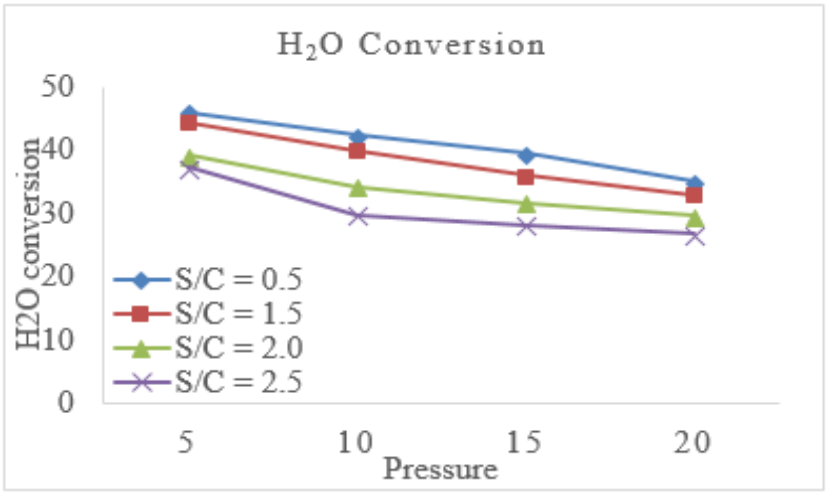

Figure 22 H_2O Conversion with Pressure(Simulation)

Syngas produced from the high-pressure reforming can easily be used in the downstream application and it reduces the compression steps in downstream applications(102,103). The simulation is done at a constant temperature of 800℃, and variable pressure and steam content. Influence of the pressure on the conversions of reactant and yield of products are shown here. The increase in the pressure is not a favorable condition for the reforming as it reduces the conversions and yields. The same trends for results are shown in the literatures(10,11,55,104,105). Le chatelier's principle can give the explanation for this, it states that "if the dynamic equilibrium is disturbed by changing the conditions, the position of equilibrium will shift in the direction of counteracting the change"(106).

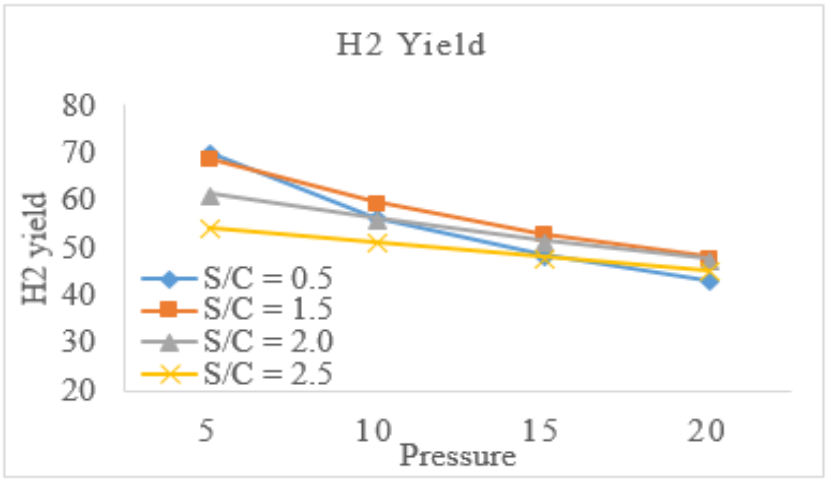

Figure 23 H_2 Yield with (Simulation)

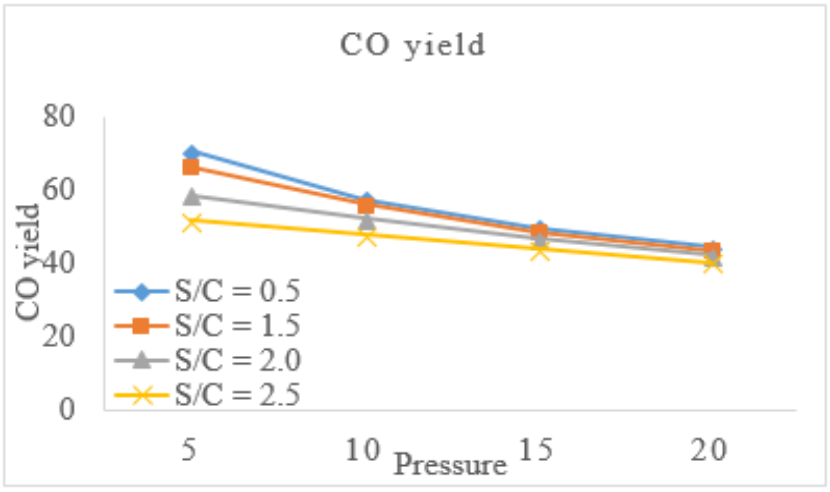

Figure 24 CO Yield with Pressure (Simulation)

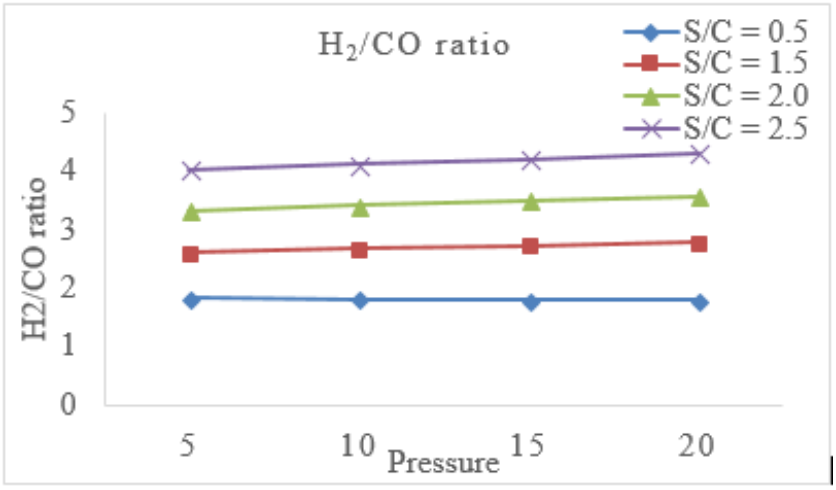

Figure 25 H_2/CO ratio with Pressure(Simulation)

CHAPTER 5
Experimental Section

5.1 Experimental Setup

The experiments were performed in "Multi-Purpose Reforming Reactor Pilot Plant". The space velocity for the gases was kept 1000 h^{-1}. The gases were supplied through mass flow controllers (MFCs) installed before the reformer reactor for particular gas. MFC controls and regulates the flow of gases.

Figure 26 Inlet Section of Reformer

The de-mineralized is supplied through a pump from the vessel to the three-stage steam generator consisting of preheater, economizer, and superheater. The superheated steam is directly supplied to the reforming reactor. The gases (CH_4 and CO_2) first routed through the sulfur guard reactor and then to the reforming reactor. The sulfur bed guard reactor has an internal and outer diameter of 20 mm and 50 mm respectively, and sulfur present in the reactant gases will be removed in this reactor.

The reforming reactor is a fixed bed downflow reactor (ID 20 mm, OD 50 mm, height 900 mm), was used to perform the reforming reactions. The reactor has four heating zones and has a total heating length of 36 inches. The setup also consists of a control panel and line heaters. Thermocouples are placed in the reactor to measure the temperature of different zones of the reformer. The reactor is also equipped with a pressure transducer that is used for the measurement of pressure. The pressure inside the reactor was maintained with a back-pressure regulator (BPR). The catalyst was kept between the layers of alumina balls in the reforming reactor. The maximum reactor volume is 5L. The maximum operating conditions for the reactor is 30 barg/up to 450℃ & 20 barg/ up to 850℃.

Figure 27 Reactor Unit

The product section of the reactor consists of product stream. The gas liquid seperator is provided at the outlet of reactor module to cool the excess water present in the product stream and also to cool the generated gases. A high-pressure gas-liquid separator is provided to separate the gases from condensed water. The outlet gases samples are collected and analysed in the mini gas chromatograph.

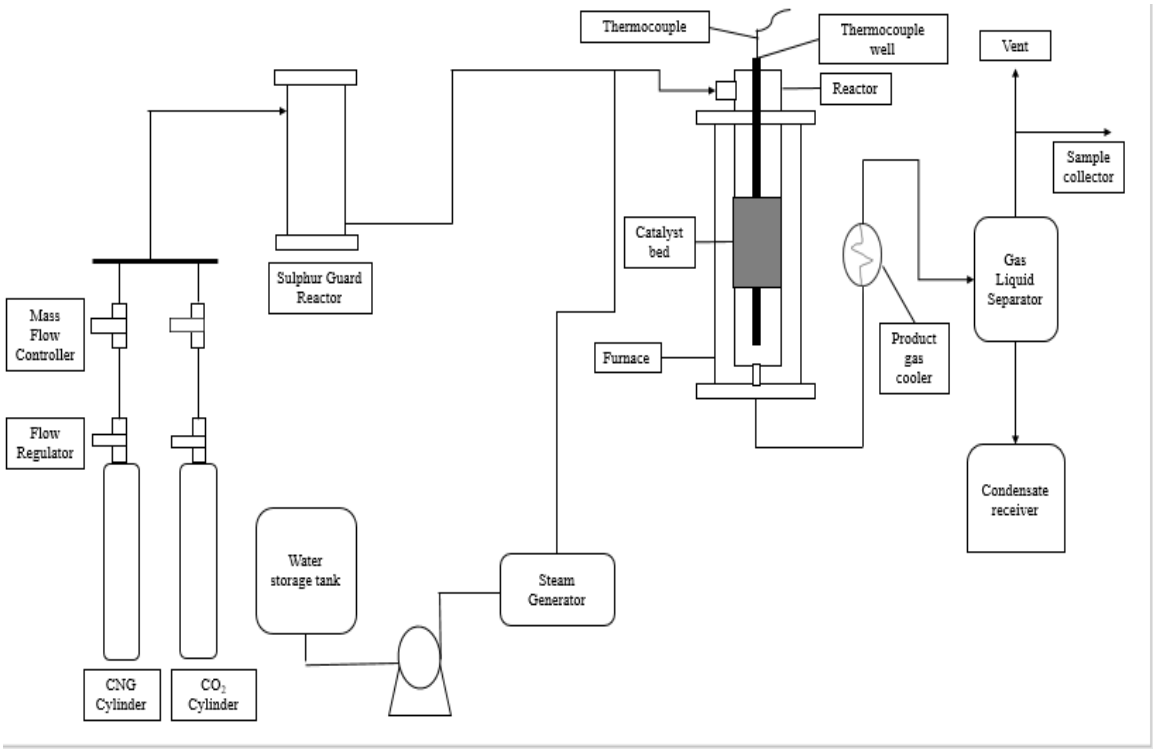

Figure 28 Layout of reforming unit

Figure 29 Multi-Purpose Reforming Unit

5.2 Experimental Conditions and procedure

The optimization of the process was conducted using commercial catalyst. The commercial catalyst that was used, is ideal for the steam reforming of natural gas. The reforming reaction was carried out over a temperature range of 600-800℃. Though combined reforming is more favorable at high temperature but due to the reactor limitation, the maximum temperature was kept 800℃. The effects of temperature, pressure and steam content were studied in our experiment. The effect of pressure was not well explained in the available literature and as the produced syngas ratio is suitable for the downstream condition, the suitability of the reforming reaction over high pressure was also studied and explained. The experiments were carried out over a pressure range of 5-20 bar, the steam to carbon ratio was also varied to evaluate the effect of steam content on the reforming reaction. The steam to carbon ratio was varied from 0.5 to 2.5.

The reforming reaction starts with the activation of the catalyst using standard activation procedure for reforming catalyst. This reforming catalyst activation procedure is a hit and trial method, the completion of the activation is indicated by the absence of steam in the exhaust. After the activation, the metal oxides will convert into the active metals.

The rate of temperature increase is 2℃/min. and dwell period are 1 min. The reforming reaction is tested for different steam content in the feed. The steam to carbon ratio was varied from 0.5 to 2.5. The total feed of gases was kept 1000 $l.h^{-1}$. The water first pumped from the water vessel to the preheater; in the preheater, the temperature of the water is increased to its boiling point. The second part of the steam generator is economizer which convert the water stream into steam. The last part of the steam generator is called superheater; it raises the temperature sufficiently to ensure that steam should not convert back to water. The superheated steam is directly supplied to the reforming reactor.

The natural gas is supplied from the NG bank to the reformer; here it is first compressed with the help of gas compressor to ensure the proper supply to the reformer. The MFC unit is installed to control the flow of the natural gas to the reformer. The natural gas first enters into the Sulphur guard reactor to remove any Sulphur content in the stream. The CO_2 gas is supplied from the cylinder located near by the reformer unit. The MFC unit is also installed to the supply

of CO_2 gas at controlled rate. The heating arrangement is provided on the CO_2 tubing to prevent the frosting on the pipes.

The streams of natural gas and CO_2 first enter into the Sulphur bed guard reactor and then in the main reforming reactor. The Sulphur bed reactor is installed to check any Sulphur content in the incoming stream because Sulphur is the main reason for the deactivation of the catalysts.

The reactor unit consists of four heating zones to maintain a uniform temperature throughout the reactor. Each heating zone is extended up to 9 cm. A layer of catalyst pellets is placed in the middle of the furnace, the catalyst layer is surrounded by the alumina balls to give it strength and stability.

The outlet stream from the reactor enters into the condenser where it is cooled down to condense any water present in the stream. The gas-liquid separator was also employed after the condenser to sperate both phases. After it, the outlet gas was collected and examined by a micro gas chromatograph to know the exact composition of the gas.

5.3 Important formulas

The performance of the catalyst is defined on the basis of conversion of CH_4 and CO_2, the maximum yield of H_2 and CO and H_2/CO ratio. The formulas for the calculations are as(13,14)-

Equation 12

$$\mathbf{CH_4\ conversion} = \frac{[CH_4]_{in} - [CH_4]_{out}}{[CH_4]_{in}} \times 100$$

Equation 13

$$\mathbf{CO_2\ conversion} = \frac{[CO_2]_{in} - [CO_2]_{out}}{[CO_2]_{in}} \times 100$$

Equation 14

$$\mathbf{H_2O\ conversion} = \frac{[H_2O]_{in} - [H_2O]_{out}}{[H_2O]_{in}} \times 100$$

Equation 15

$$H_2\ \mathbf{yield} = \frac{[H_2]_{out}}{2 \times [CH_4]_{in} + [H_2O]_{in}} \times 100$$

Equation 16

$$\mathbf{CO\ yield} = \frac{[CO]_{out}}{[CH_4]_{in} + [CO_2]_{in}} \times 100$$

Equation 17

$$\frac{H_2}{CO}\ \text{ratio} = \frac{\text{mole of } H_2 \text{ produced}}{\text{mole of CO produced}}$$

5.4 Activation Procedure of catalyst

The commercial catalyst was activated as per the standard activation procedure followed for the reforming catalyst at the IOCL R&D center.

1. Pressurize the system to 5 bars with H_2.
2. Set H_2 flow rate 843 SLPH.
3. Heat up the reactor from 30℃ to 150℃ @ 34.3℃/h.
4. Hold at 150℃ for 2 hr.
5. Heat up the reactor from 150℃ to 300℃ @ 30℃/h.
6. At these conditions hold for 1 hr.
7. Increase H_2 flow rate to 1673 SLPH.
8. Heat up the reactor from 300℃ to 450℃ @ 30℃/h.
9. At these conditions hold for 1 hr.
10. Increase H_2 flow rate to 2496 SLPH from 1673 SLPH.
11. At these conditions hold for 8 hr.
12. Increase the reactor from 450℃ to 650℃ @ 50℃/h.
13. Maintain this condition for 2 hr.

The completion of the activation is shown by the absence of water steam at the exhaust of the reformer.

CHAPTER 6
Results & Discussion

6.1 Characterization of Catalyst

The analysis of the catalyst was done with the help of SEM, XRD, TGA, EDX method. The mapping of the catalyst was also done to know the distribution of metal components on the surface of the catalyst. The BET surface area analysis of the commercial catalyst shows the specific surface area equal to 29 m^2/g. The results for characterization are as follows

6.1.1 SEM Result

The SEM images of the commercial catalyst show that the active metals are greatly distributed over the surface of the support material. The SEM images were taken at the different resolution for careful study of the catalyst and all of them shows a good interaction between the two active metals and the support. The active metals are cylindrical in shape and uniformly distributed over the support surface.

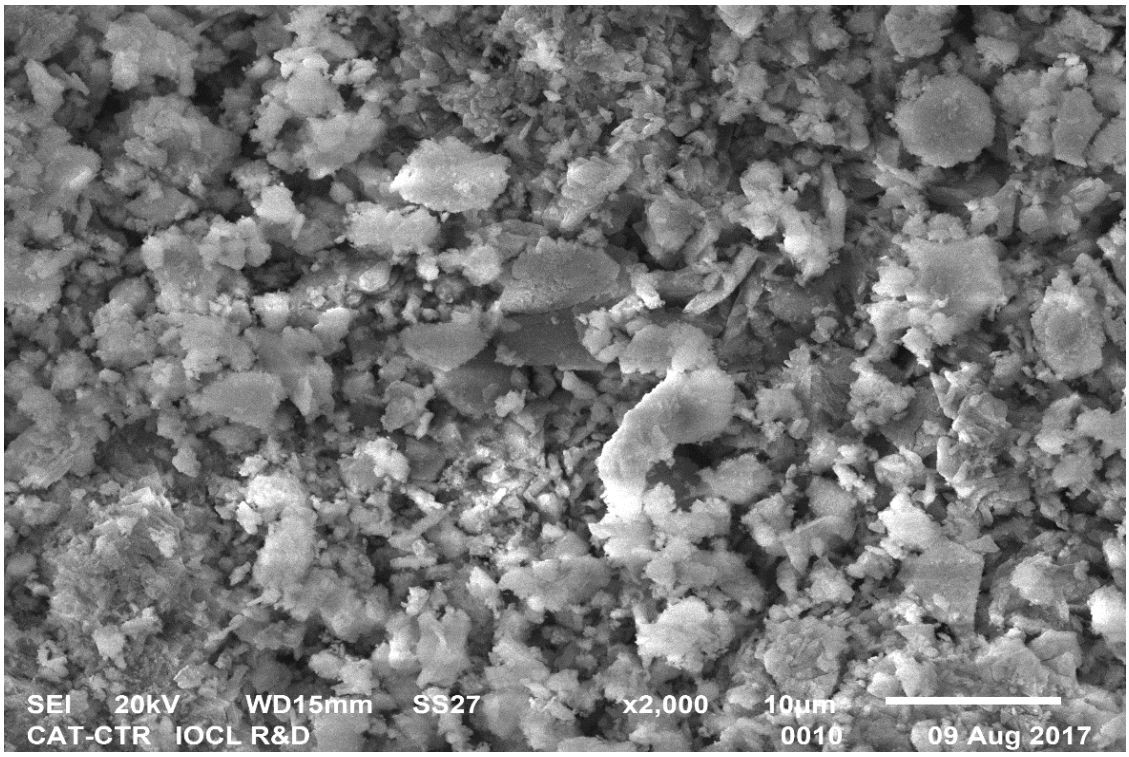

Figure 30 SEM Result

6.1.2 EDX Result

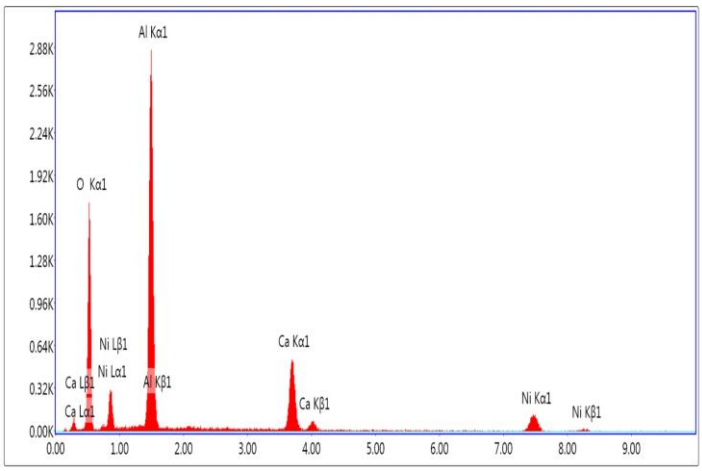

Element	Weight %	Atomic %
O K	32.46	50.42
AlK	39.47	36.36
CaK	6.81	4.22
NiK	21.26	9.00

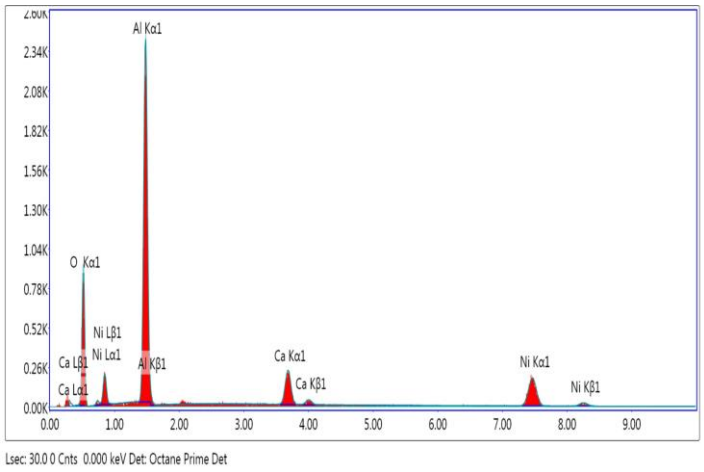

Element	Weight %	Atomic %
O K	32.46	50.42
AlK	39.47	36.36
CaK	6.81	4.22
NiK	21.26	9.00

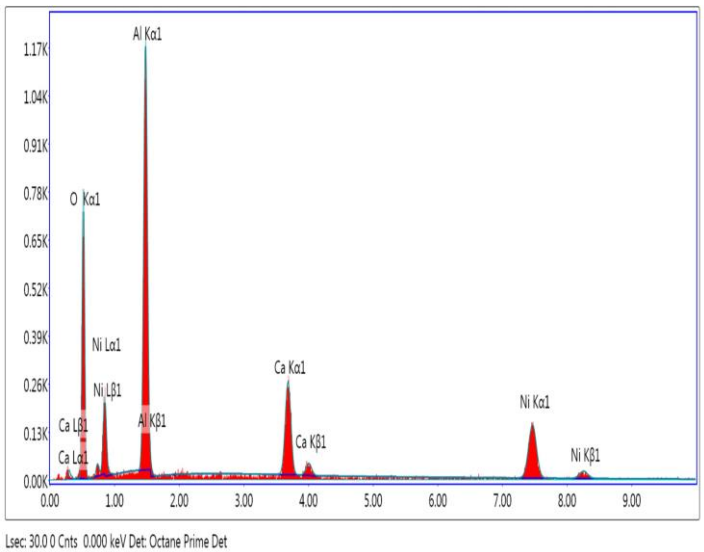

Element	Weight %	Atomic %
O K	38.55	58.77
AlK	28.09	25.39
CaK	10.29	6.26
NiK	23.07	9.58

Figure 31 EDX Results

The EDX results of different spots on the catalyst surface show the presence of Ni, Ca, Al and O on the surface. From XRD results it is evident that the catalyst is composed of nickel and calcium metal on the surface of alumina support.

6.1.3 XRD Result

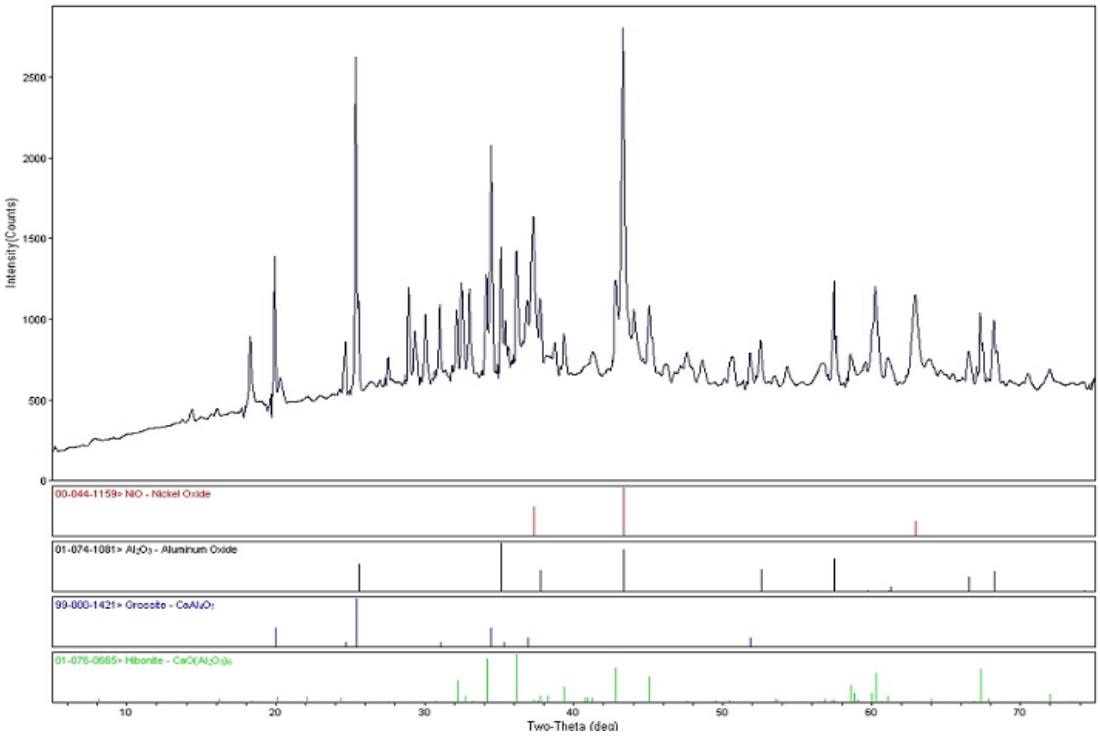

Figure 32 XRD Spectrum

The XRD spectrum of commercial catalyst showed the presence of peaks matching with Ni Oxide, Al Oxide Ca-Al-Based oxides (different forms). The XRD result showed the formation of a complex of Calcium and Alumina.

6.1.4 TGA Result

The TGA analysis of sample was done under the inert atmosphere. The change in the mass of the sample with increase in temperature up to 800℃ was noted. The line in the TGA curve shows the change in the mass of the sample with respect to temperature. The change in mass at initial stage is may be due to the moisture content in the sample. The intermediate change is attributed to some unstable hydroxides and oxides present in the sample. The overall change in the mass is very low and it shows that the catalyst is stable at a temperature of 800℃.

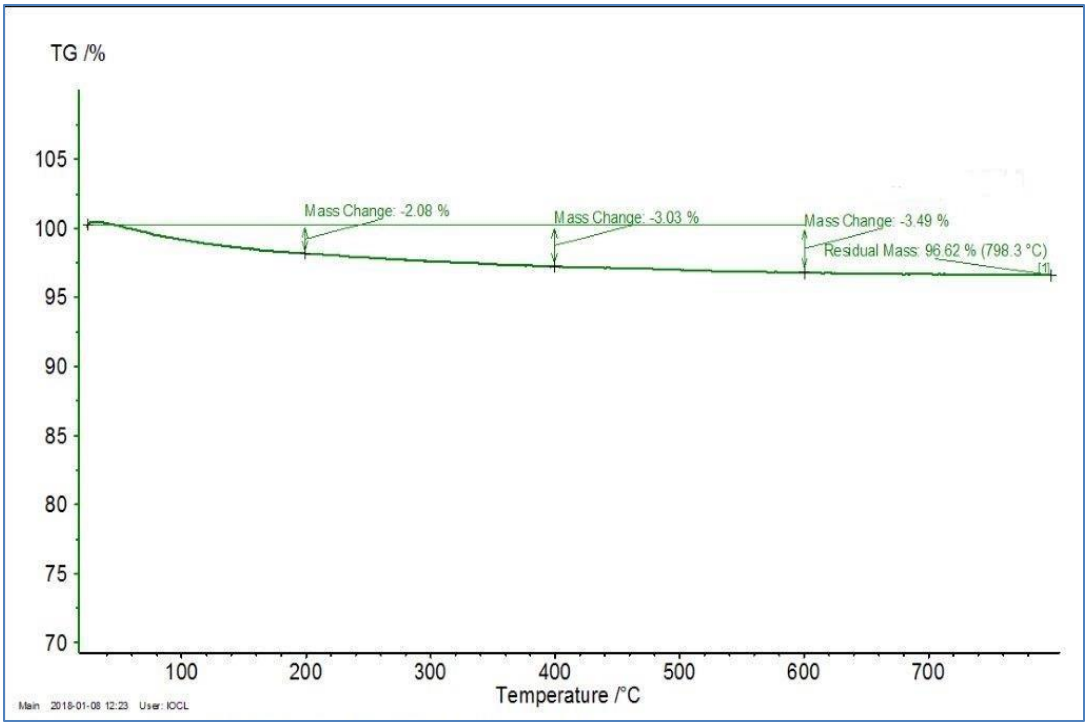

Figure 33 TGA Analysis

6.2 Experiment Conditions and Procedure

The first set of experiment was to determine the effect of temperature and the steam content on the reforming results. The reactor pressure was 5 bars in the first set. The temperature of the reactor was raised from 650℃ to 800℃ and its effects on the conversion and yield were studied. The steam to carbon ratio was also varied from 0.5 to 2.5. The time on stream(TOS) was 2 hrs.

6.3 Experimental Results

6.3.1 Effects of Temperature & Steam Content

The CH_4 conversion increases with increase in both temperature and amount of steam content as in case of simulation (Figure 34). CH_4 is the main reactant in both steam and dry reforming and the cumulative effect of both reactions resulted in an increased CH_4 conversion. CH_4 conversion increase with the temperature because of the endothermic nature of both the reaction(12–14). At starting temperature condition, the steam reforming was the dominating reaction and the higher temperature ranges the dry reforming became

more dominating. The methane conversion will always increase with an increase in temperature and steam content; both steam content and temperature favor methane conversion(58,58,64).

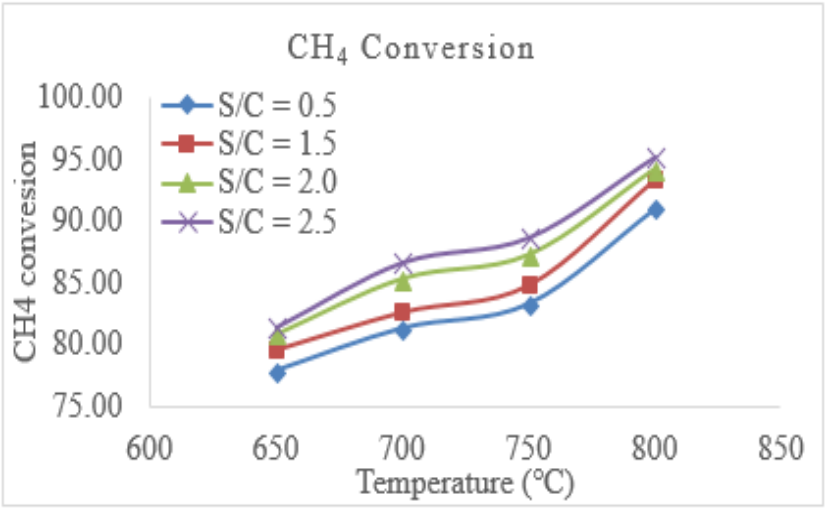

Figure 34 Methane Conversion

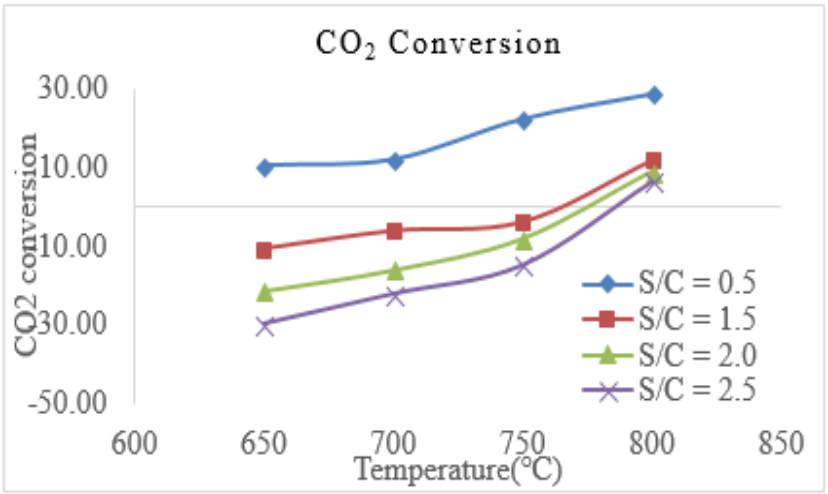

Figure 35 CO_2 Conversion

The CO_2 conversion is also very much dependent on the temperature and steam content. The CO_2 conversion increase with an increase in temperature because both dry reforming and reverse water gas shift reaction are more favorable at high temperature due to their high endothermic nature(11–13,62). The CO_2 conversion always decreases with increase in S/C ration i.e. amount of steam because the steam reforming is always more preferable than dry reforming because of its lower

endothermic nature and stable nature of CO_2(13). The water gas shift reaction also plays a major role here because it increases with steam content and water molecules react with CO and produce CO_2. So, at a lower temperature, a negative CO_2 conversion is observed. So, it can be concluded that higher the amount of steam added, higher the contribution of SRM and WGS. So, low steam content and high temperature are favorable for the CO_2 conversion. The highest CO_2 conversion (19.14%) was obtained at a high temperature (800℃) and low S/C ratio (0.5).

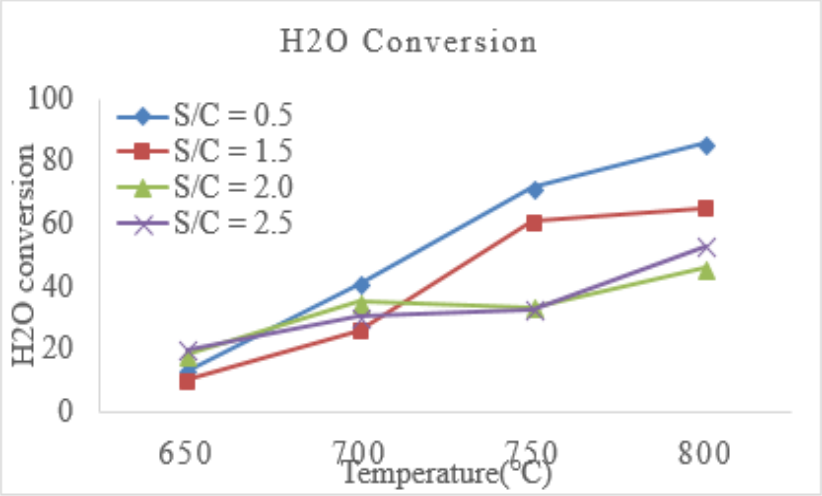

Figure 36 H_2O Conversion

The experimental H_2O conversion follows the same trend as shown in the simulation. The H_2O conversion increase with an increase in the steam content at a lower temperature because the steam reforming and WGS reaction are dominant at a lower temperature. At higher temperature, the H_2O conversion decreases with increase in steam content because of the occurrence of dry reforming and RWGS reactions.

The experiment results show the same trend as that of simulation. The H_2 yield always increases with increase in both temperatures. At lower temperature, both steam reforming and WGS reactions are responsible for hydrogen production. Both the reaction will be favorable for hydrogen production and the hydrogen yield increases(21). But at a higher temperature, the increase in steam content doesn't increase the H_2 yield because at this stage the dry reforming will be more dominant

which yields less H_2. The RWGS reaction is also dominant at the high temperature and it consumes the H_2 generated.

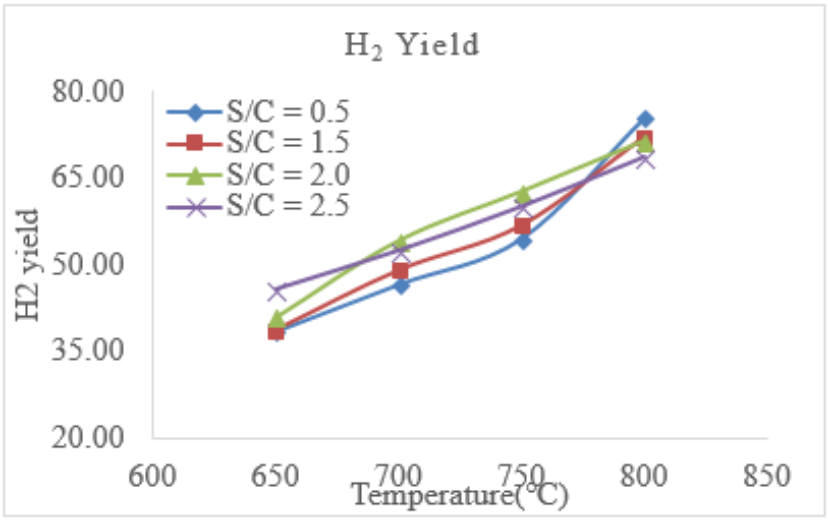

Figure 37 H_2 Yield

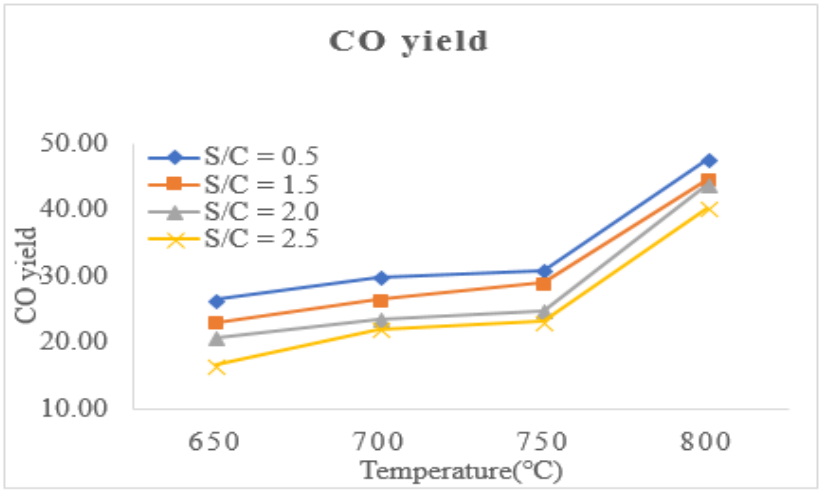

Figure 38 CO Yield

The CO yield is also dependent on both temperature and steam content. At lower temperature conditions the WGS reaction in more favorable and it results in lower CO yield because the produced CO reacts with water molecules and produce CO_2 and hydrogen. The increase in steam content also favors the water gas shift reaction, so the CO yield decreases with increase in steam content. At higher temperature conditions the RWGS reaction is favored, so the amount of CO increases with

increase in temperature. The favorable conditions for the CO yield are high temperature and low steam content because at low temperature the water gas shift reaction will be favorable which cause the reduction in CO yield. At high-temperature conditions, the reverse water gas reaction will increase the CO yield. Increase in steam content will also favor the WGS; so, the high CO yield will be obtained at the low steam content.

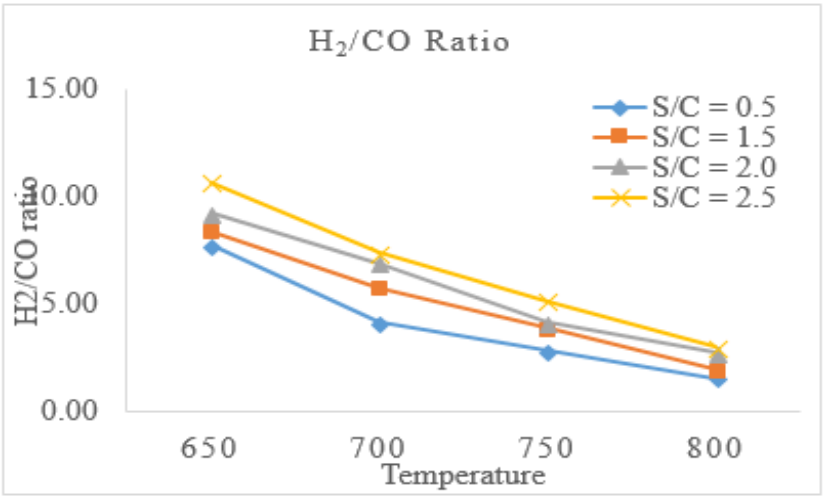

Figure 39 H_2/CO Ratio

H_2/CO ratio is dependent on the hydrogen and CO produced. At lower temperature regions higher H_2/CO ratio is obtained because water gas shift reaction was more favorable. WGS reaction resulted in the increased amount of hydrogen and decreased the amount of CO, and the addition of steam always increases the H_2 yield, so at a lower temperature and higher S/C ratio high H_2/CO ratio is obtained. As the temperature increases the reverses water gas shift reaction becomes more favorable and the amount of CO increases with increase in temperature, the lower H_2/CO ratio is obtained at a higher temperature.

The effect of temperature and steam content on the tri-reforming shows that the reaction is dependent on both the temperature and steam content. The conversion of both methane and CO_2 increase with an increase in the temperature. The methane conversion increase with an increase in steam conversion but the CO_2 conversion decrease with increase in the steam content.

The hydrogen yields also increase with an increase in both temperature and steam content but at high temperature the rate of H_2 yield dampens with increase in steam content. H_2/CO ratio decreases with increase in temperature but increases with an increase in steam content.

All the results are in good agreement with the available literature(9–11,107)

6.3.2 Effect of Pressure and Steam Content

To evaluate the effect of pressure on the reforming reaction; the temperature of the reformer was kept content at 800℃ and pressure was varied from 5 bars to 20 bars. The steam content was also varied to check for its effect combined with pressure. The S/C (Steam to carbon ratio) was varied from 0.5 to 2.5. All the other conditions were kept as same as that of the first study. The Le chatelier's principle plays an important role in the study. As per the le chatelier's principle when we try to disturb the equilibrium of a reaction either by changing temperature and pressure, the equilibrium will shift in the direction of release of the effect(106,108). In our reaction, the number of reactants is 4 and number of the product is 8, so as we increase the pressure the equilibrium will disturb and to release this effect the product concentration will decrease(13).

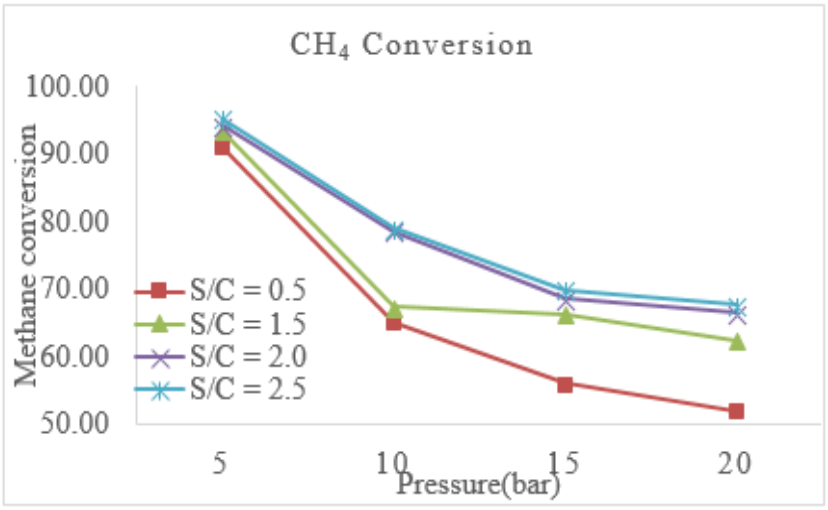

Figure 40 Methane conversion with pressure

Methane conversion decrease with increase in the pressure because the reforming reaction is basically a low-pressure reaction so as the pressure increases the conversion of methane decreases. The methane conversion increase with an

increase in the steam content because methane is main content in both steam and dry reforming, and due to both these reactions the conversion of methane increases. The conversion of methane decreases rapidly with increase in the pressure because of unfavorable conditions for the reaction. At high steam content, the decrease is not so rapid because of both steam and dry reforming. So, the high temperature and low pressure are required for the high methane conversion.

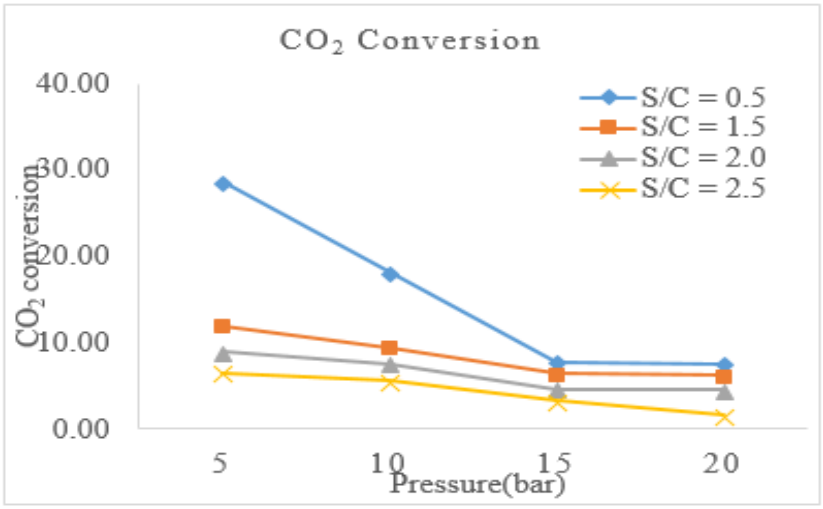

Figure 41 CO_2 conversion with pressure

The CO_2 conversion also decreases with increase in pressure. CO_2 is the main reactant in a dry reforming reaction which is only favorable at low-pressure condition so as the pressure increases the CO_2 conversion decreases. The CO_2 conversion also becomes very low with a further increase in pressure because at that state the water gas shift reaction will produce CO_2 and conditions will become unfavorable for the dry reforming conditions. The CO_2 conversion also decreases with increase in the steam content because the steam reforming will become more favorable at that state. So, high temperature, low pressure, and low steam to carbon ratio are preferred for high CO_2 conversion.

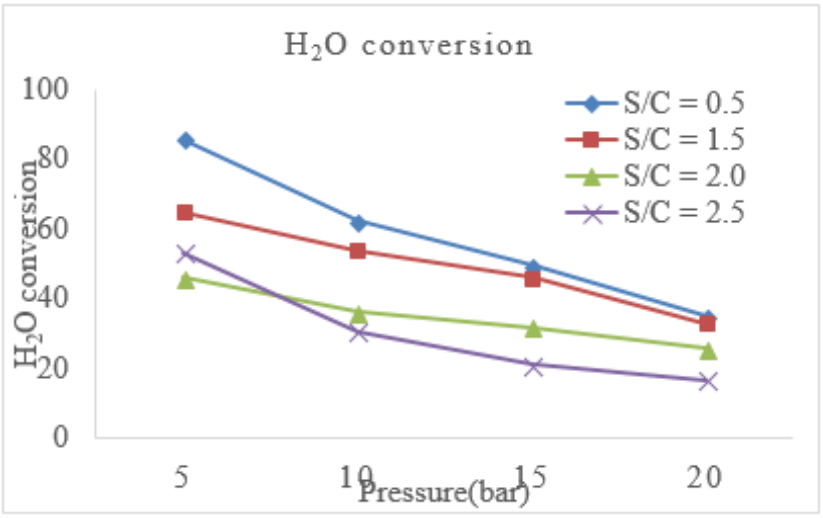

Figure 42 H_2O conversion with pressure

H_2O conversion is shown in Figure 42 has the same trend as of the simulation. The H_2O conversion decrease with increase in the pressure because both the steam and dry reforming are not favorable at the high pressure. WGS shift reaction is also not favorable at high-pressure conditions. So, for the high H_2O conversion low S/C ratio, high temperature and low pressure are the ideal conditions for the H_2O conversion.

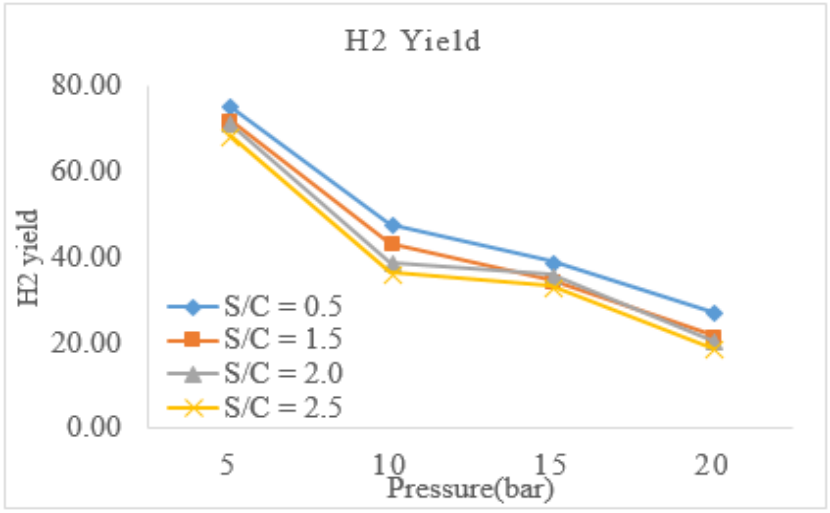

Figure 43 Hydrogen yield with pressure

Hydrogen yield also decreases with increase in pressure of the reformer unit and shows the similar trend as that of simulation. The reforming reaction is a low-

pressure reaction so the hydrogen yield decreases with increase in pressure. The hydrogen yield at high steam contents (steam to carbon ratio = 2.0&2.5), the hydrogen yields almost remain equal and follow the same trend. The maximum hydrogen yield is obtained at high temperature, low pressure, and moderate steam content.

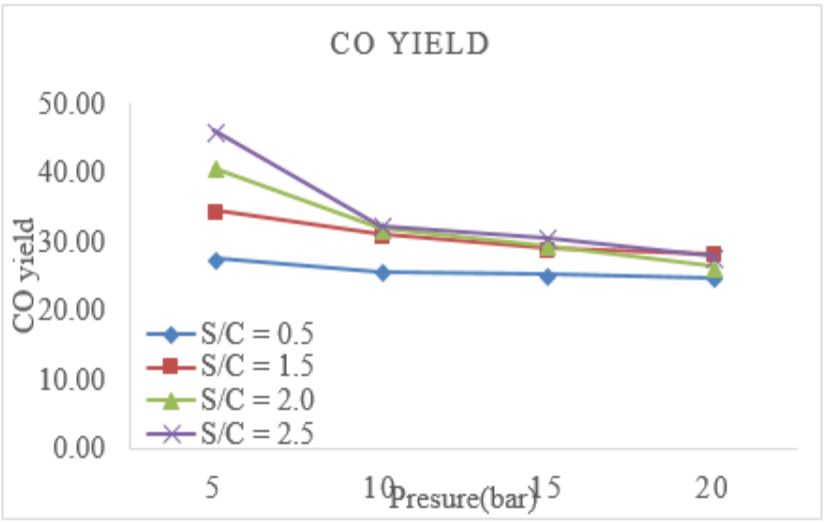

Figure 44 CO yield with pressure

The CO yield also decreases with increase in the pressure but the variation in CO yield is more with high steam content. At lower S/C ratio, the decrease in CO yields with pressure is not as much as with high steam to carbon ratio. The low CO yield at high temperature may be due to the occurrence of reverse water gas shift reactions. The most preferred conditions for the highest CO yield is high temperature, low pressure and high S/C ratio.

H_2/CO ratio also decreases rapidly with increase in the pressure. The H_2 yield and CO yield also decrease with increase in the pressure, so H_2/CO ratio also decreases. The reduction in CO yield is not as rapid as a reduction in H_2 yield, so the H_2/CO ratio decrease with the increase in the pressure. The reduction in H_2/CO ratio at high steam-to-carbon ratio is not rapid as with low steam-to-carbon ratio because at high S/C ratio more steam is present to generate hydrogen.

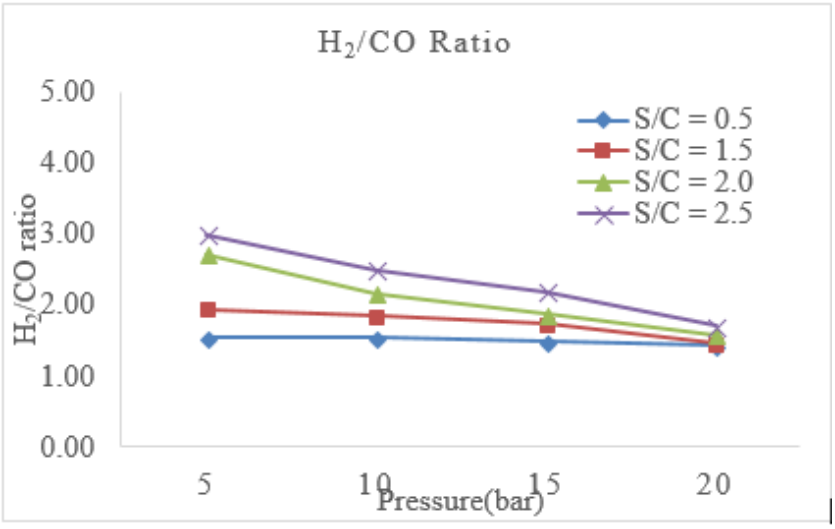

Figure 45 H_2/CO Ratio with pressure

The increase in the pressure is not favorable for the reforming reactions as per the study. The increase in pressure results in a decrease in conversion of methane & CO2, the yield of hydrogen & CO, and H2/CO ratio. The Le chatelier's principle describes the effect of the pressure on the reaction. The reforming reaction is a low pressure and high-temperature reaction.

6.4 Energy balance

The energy balance is done for the most optimized condition. In energy balance calculation the total energy given to the system and total available energy in the form of hydrogen is being calculated.

- Energy supplied to the methane and CO_2-

$$m_{CH4} = 0.4818\text{kg}, m_{CO2} = 0.736\text{ kg}$$

$$C_p = \alpha+\beta T+\gamma T^2+\delta T^3+\varepsilon T^4$$

$$Q_{in} = mC_{p,\,CH4}\Delta T + m_{Cp,\,CO2}\,\Delta T$$

$$C_{p,\,CH4} = 4.595\text{ kJ/kg}, C_{p,\,CO2} = 1.25\text{ kJ/kg}$$

$$Q_{in} = 2429.31\text{ kJ}$$

- Energy supplied to the water steam

P= 5bar, T_{sat} = 158.919℃, $T_{superheated\ steam}$ = 210℃

Latent heat of vaporization = 2085.6 kJ/kg

$$Q_{in} = mC_p\Delta T$$

$$Qin = 11{,}068.08 \text{ kJ}$$

- Total heat supplied = 13,497.04 kJ
- Total energy content of hydrogen produced

$$m = 0.1573 \text{ kg}$$

$$\text{Energy of hydrogen} = \text{Mass} \times \text{Energy content per kg}$$

$$\text{Energy of Hydrogen} = 18000 \text{ kJ}$$

So, from energy balance it is clear that we have a net gain of energy and we are generating clean energy at the expanse of two major greenhouse gases. The net energy balance shows that at the optimized condition this reforming process is beneficial.

CHAPTER 7
Summary & Conclusion

7.1 Summary

Tri-reforming of natural gas was performed with the use of steam and carbon dioxide. Oxygen was not allowed to use due to safety measure. The reforming reactions were performed under a constant flow rate of 1000 $l.h^{-1}$. The temperature of the reaction was varied from 650℃ to 800℃, the pressure of the reformer was also varied from 5bar to 20 bars. The steam to carbon ratio of the reaction was varied from 0.5 to 2.50. The steam to carbon ratio was calculated on the basis of mole numbers of the reactants. The time of stream was taken 2 hrs. The product gases were collected and examined with the help of mini gas chromatograph. The reforming catalyst used was a commercial catalyst. The analysis of the commercial catalyst was done with the help of XRD, SEM-EDX, and TGA. The BET surface area analysis of the catalyst was also done. The increase in temperature is favorable for the reforming reaction but the increase in pressure in unfavorable as it decreases the conversion of gases and yield of hydrogen generation. The addition of steam in the reaction at lower temperature leads to (a) decrease in the CO_2 conversion (b) increase in H_2 yield and decrease in CO yield (c) increase in H_2/CO ratio.

Although both steam and dry reforming are favorable at high temperature and steam reforming should be more dominant because of its lower endothermic nature. So, the addition of steam at high temperature should have favored the H_2O conversion and high H_2 yield but the experiment shows that dry reforming and RWGS reactions are more dominant at the high-temperature conditions.

There might be three reasons for the less H_2 yield at high temperature and high steam content-

a) The occurrence of dry reforming which yields less hydrogen.
b) The occurrence of RWGS reaction which consumes the generated hydrogen.
c) The extra steam is added over the fixed amount of CH_4 and CO_2 at inlet feed. (14)

The increase in the pressure is not at all favorable for hydrogen generation as it reduces the yield of hydrogen.

7.2 Conclusion

The results of the reforming reaction show the following conclusions-

1. High temperature and low pressure are the preferred conditions for the reforming reaction.
2. The addition of steam results in low CO_2 conversion and high hydrogen generation.
3. The increase in pressure shows a decrease in conversion of both methane & CO_2 and lower the yield of both hydrogen and CO.
4. The addition of steam results in high H_2/CO ratio.
5. At high temperature, the H_2/CO ratio for all the conditions become almost equal to 2.
6. Maximum CH_4 conversion 95.24% was obtained at 800℃, 5 bar and S/C = 2.50, maximum CO_2 conversion 28.65% was obtained at 800℃, 5 bar and S/C = 0.50.
7. Both Maximum H_2 yield 75.48% and CO yield 47.63% were obtained at 800℃, 5 bars with S/C ration of 0.50.
8. All the results show that proper control of feed and temperature is required for the maximum hydrogen yield because steam reforming, dry reforming, and RWGS reaction are endothermic in nature and a compromise between these reactions is required for the high hydrogen yield at the high-temperature zone.
9. Our tri-reforming is a complex multi-reaction system where various reactions (SRM, DRM, WGS, RWGS) occur simultaneously depending upon the temperature and feed composition.

References

1. Fuels - Higher and Lower Calorific Values [Internet]. [cited 2018 May 30]. Available from: https://www.engineeringtoolbox.com/fuels-higher-calorific-values-d_169.html

2. Hydrogen and Syngas Production and Purification Technologies.pdf [Internet]. [cited 2018 May 24]. Available from: http://197.14.51.10:81/pmb/CHIMIE/Hydrogen%20and%20Syngas%20Production%20and%20Purification%20Technologies.pdf

3. Bohmer N, Roussiere T, Schunk MK and SA. Valorisation of Glycerol as Renewable Feedstock: Comparison of the Exploration of Chemical Transformation Methods Aided by High Throughput Experimentation [Internet]. Combinatorial Chemistry & High Throughput Screening. 2012 [cited 2018 May 26]. Available from: http://www.eurekaselect.com/76040/article

4. Laurendeau NM. Heterogeneous kinetics of coal char gasification and combustion. Prog Energy Combust Sci. 1978 Jan 1;4(4):221–70.

5. Roussière TL. Catalytic Reforming of Methane in the Presence of CO2 and H2O at High Pressure. :238.

6. Ghoneim SA, El-Salamony RA, El-Temtamy SA. Review on Innovative Catalytic Reforming of Natural Gas to Syngas. World J Eng Technol. 2016;04(01):116–39.

7. Partial oxidation of methane over Ni0/La2O3 bifunctional catalyst II: Global kinetics of methane total oxidation, dry reforming and partial oxidation | Sci-napse | Academic search engine for paper [Internet]. Synapse. [cited 2018 May 26]. Available from: https://scinapse.io/papers/1964593821

8. The catalytic stability of TiO2-shell/Ni-core catalysts for CO2 reforming of CH4 | Sci-napse | Academic search engine for paper [Internet]. Scinapse. [cited 2018 May 26]. Available from: https://scinapse.io/papers/2088034900

9. Li Y, Wang Y, Zhang X, Mi Z. Thermodynamic analysis of autothermal steam and CO2 reforming of methane. Int J Hydrog Energy. 2008 May;33(10):2507–14.

10. Özkara-Aydınoğlu Ş. Thermodynamic equilibrium analysis of combined carbon dioxide reforming with steam reforming of methane to synthesis gas. Int J Hydrogen Energy. 2010 Dec;35(23):12821–8.

11. Soria MA, Mateos-Pedrero C, Guerrero-Ruiz A, Rodríguez-Ramos I. Thermodynamic and experimental study of combined dry and steam reforming of methane on Ru/ ZrO2-La2O3 catalyst at low temperature. Int J Hydrogen Energy. 2011 Nov;36(23):15212–20.

12. Li Z, Kathiraser Y, Kawi S. Facile Synthesis of High Surface Area Yolk–Shell Ni@Ni Embedded SiO2 via Ni Phyllosilicate with Enhanced Performance for CO2 Reforming of CH4. ChemCatChem. 7(1):160–8.

13. Hu YH, Ruckenstein E. An optimum NiO content in the CO<Subscript>2</Subscript> reforming of CH<Subscript>4</Subscript> with NiO/MgO solid solution catalysts. Catal Lett. 1996 Sep 1;36(3–4):145–9.

14. Choudhary VR, Rajput AM. Simultaneous Carbon Dioxide and Steam Reforming of Methane to Syngas over NiO−CaO Catalyst. Ind Eng Chem Res. 1996 Jan 1;35(11):3934–9.

15. Vr C, Kc M. CO2 reforming of methane combined with steam reforming or partial oxidation of methane to syngas over NdCoO3 perovskite-type mixed-metal-oxide catalyst. Appl Energy. 2006;83(9):1024–32.

16. 99c02f5f43b3946789b3d2075bb544e743f5.pdf [Internet]. [cited 2018 May 26]. Available from: https://pdfs.semanticscholar.org/b7d7/99c02f5f43b3946789b3d2075bb544e743f5.pdf

17. Noronha FB, Shamsi A, Taylor C, Fendley EC, Stagg-Williams S, Resasco DE. Catalytic Performance of Pt/$ZrO_2$and Pt/Ce-ZrO_2 Catalysts on CO_2 Reforming of CH_4 Coupled with Steam Reforming or Under High Pressure. Catal Lett. 2003 Sep 1;90(1–2):13–21.

18. Song C, Pan W. TRI-REFORMING OF METHANE: A NOVEL CONCEPT FOR SYNTHESIS OF INDUSTRIALLY USEFUL SYNTHESIS GAS WITH DESIRED H2/CO RATIOS USING CO2 IN FLUE GAS OF POWER PLANTS WITHOUT CO2 SEPARATION. :4.

19. Choudhary VR, Rajput AM, Prabhakar B. Energy efficient methane-to-syngas conversion with low H_2/CO ratio by simultaneous catalytic reactions of methane with carbon dioxide and oxygen. Catal Lett. 1995 Sep 1;32(3–4):391–6.

20. Steam and oxysteam reforming of methane to syngas over Cox Ni1−x O supported on MgO precoated SA-5205 - Choudhary - 2001 - AIChE Journal - Wiley Online Library [Internet]. [cited 2018 May 26]. Available from: https://onlinelibrary.wiley.com/doi/pdf/10.1002/aic.690470715

21. Tri-reforming of methane to syngas over Ni/Al2O3 — Thermal distribution in the catalyst bed - [PDF Document] [Internet]. documents.site. [cited 2018 May 29]. Available from: https://vdocuments.site/documents/tri-reforming-of-methane-to-syngas-over-nial2o3-thermal-distribution-in.html

22. Moon DJ, Kang JS, Nho WS, Kim D-H, Lee SD, Lee BG. Ni-based catalyst for tri-reforming of methane and its catalysis application for the production of syngas [Internet]. US20080260628A1, 2008 [cited 2018 May 29]. Available from: https://patents.google.com/patent/US20080260628A1/en

23. Amin M. APCChE 2015-Tri-reforming of methane. [cited 2018 May 29]; Available from: http://www.academia.edu/14966955/APCChE 2015 Tri-reforming of methane

24. Song-MASc_Thesis3.pdf [Internet]. [cited 2018 May 29]. Available from: https://uwspace.uwaterloo.ca/bitstream/handle/10012/5375/Song-MASc_Thesis3.pdf?sequence=1

25. Thermodynamic Analyses of Tri-reforming Reactions To Produce Syngas - Energy & Fuels (ACS Publications) [Internet]. [cited 2018 May 29]. Available from: https://pubs.acs.org/doi/abs/10.1021/ef500084m

26. What is Syngas - BioFuel Information [Internet]. [cited 2018 May 29]. Available from: http://biofuel.org.uk/what-is-syngas.html

27. 11_chapter no. 02.pdf [Internet]. [cited 2018 May 27]. Available from: http://shodhganga.inflibnet.ac.in/bitstream/10603/153840/11/11_chapter%20no.%2002.pdf

28. Synthesis gas, (syngas), producer gas use in gas engines [Internet]. Clarke Energy. [cited 2018 May 29]. Available from: https://www.clarke-energy.com/synthesis-gas-syngas/

29. What is SynGas? [Internet]. AZoCleantech.com. 2013 [cited 2018 May 29]. Available from: https://www.azocleantech.com/article.aspx?ArticleID=377

30. De Tissera S, Köpke M, Simpson SD, Humphreys C, Minton NP, Dürre P. Syngas Biorefinery and Syngas Utilization. Adv Biochem Eng Biotechnol. 2017 Jun 20;

31. Tan JS, Danh HT, Singh S, Truong QD, Setiabudi HD, Vo D-VN. Syngas Production from CO 2 Reforming and CO 2 -steam Reforming of Methane over Ni/Ce-SBA-15 Catalyst. IOP Conf Ser Mater Sci Eng. 2017;206(1):012017.

32. Bae JW, Kim AR, Baek S-C, Jun K-W. The role of CeO2–ZrO2 distribution on the Ni/MgAl2O4 catalyst during the combined steam and CO2 reforming of methane. React Kinet Mech Catal. 2011 Sep 7;104(2):377–88.

33. Guo J, Lou H, Zhu Y, Zheng X. La-based perovskite precursors preparation and its catalytic activity for CO2 reforming of CH4. Mater Lett. 2003 Oct 1;57(28):4450–5.

34. Belhadi A, Trari M, Rabia C, Cherifi O. Methane Steam Reforming on Supported Nickel Based Catalysts. Effect of Oxide ZrO2, La2O3 and Nickel Composition. Open J Phys Chem. 2013 May 23;03:89.

35. Kalai DY, Stangeland K, Li H, Yu Z. The effect of La on the hydrotalcite derived Ni catalysts for dry reforming of methane. Energy Procedia. 2017 Dec;142:3721–6.

36. Xu Y, Chun DH, Jang JH, Demura M, Wee DM, Hirano T. Catalytic Activity of Oxidation-Reduction Pre-Treated Ni_3Al for Methane Steam Reforming. Adv Mater Res. 2010 Jan;89–91:645–50.

37. Bartholomew CH. Mechanisms of catalyst deactivation. Appl Catal Gen. 2001 Apr 30;212(1):17–60.

38. Vita A, Italiano C, Fabiano C, Laganà M, Pino L. Influence of Ce-precursor and fuel on structure and catalytic activity of combustion synthesized Ni/CeO2 catalysts for biogas oxidative steam reforming. Mater Chem Phys. 2015 Aug 1;163:337–47.

39. Pino L, Vita A, Laganà M, Recupero V. Hydrogen from biogas: Catalytic tri-reforming process with Ni/LaCeO mixed oxides. Appl Catal B Environ. 2014 Apr 27;148–149:91–105.

40. Vita A, Pino L, Cipitì F, Laganà M, Recupero V. Biogas as renewable raw material for syngas production by tri-reforming process over NiCeO2 catalysts: Optimal operative condition and effect of nickel content. Fuel Process Technol. 2014 Nov 1;127:47–58.

41. Garbarino G, Chitsazan S, Phung TK, Riani P, Busca G. Preparation of supported catalysts: A study of the effect of small amounts of silica on Ni/Al2O3 catalysts. Appl Catal Gen. 2015 Sep 25;505:86–97.

42. Okura K, Okanishi T, Muroyama H, Matsui T, Eguchi K. Ammonia Decomposition over Nickel Catalysts Supported on Rare-Earth Oxides for the On-Site Generation of Hydrogen. ChemCatChem. 8(18):2988–95.

43. Ayodele BV, Hossain MA, Shahirah MNN, Khan MR, Cheng CK. Synthesis, characterization and catalytic performance of samarium sesquioxide supported cobalt catalyst for methane dry reforming to syngas.

44. Shahirah MNN, Abdullah S, Gimbun J, Ng YH, Cheng CK. A study on the kinetics of syngas production from glycerol over alumina-supported samarium–nickel catalyst. Int J Hydrogen Energy. 2016;41(25):10568–10577.

45. Zhao Y, Kang Y, Li H, Li H. CO2 conversion to synthesis gas via DRM on the durable Al2O3/Ni/Al2O3 sandwich catalyst with high activity and stability. Green Chem [Internet]. 2018 Apr 28 [cited 2018 May 29]; Available from: http://pubs.rsc.org/en/content/articlelanding/2018/gc/c8gc00743h

46. Characteristics of activated carbon modified with alkaline KMnO 4 and its performance in catalytic reforming of greenhouse gases CO 2 /CH 4 [Internet]. [cited 2018 May 29]. Available from:

https://www.researchgate.net/publication/317252620_Characteristics_of_activated_carbon_modified_with_alkaline_KMnO_4_and_its_performance_in_catalytic_reforming_of_greenhouse_gases_CO_2_CH_4

47. An experimental and theoretical investigation of the biogas dry reforming reaction over Ni supported on modified with CeO2 or La2O3 zirconia catalysts [Internet]. ResearchGate. [cited 2018 May 26]. Available from: https://www.researchgate.net/publication/305333071_An_experimental_and_theoretical_investigation_of_the_biogas_dry_reforming_reaction_over_Ni_supported_on_modified_with_CeO2_or_La2O3_zirconia_catalysts

48. Koubaissy B, Pietraszek A, Roger AC, Kiennemann A. CO2 reforming of methane over Ce-Zr-Ni-Me mixed catalysts. Catal Today. 2010 Nov 17;157(1):436–9.

49. Yao L, Shi J, Xu H, Shen W, Hu C. Low-temperature CO2 reforming of methane on Zr-promoted Ni/SiO2 catalyst. Fuel Process Technol. 2016 Apr 1;144:1–7.

50. Nickel on alumina catalysts for the production of hydrogen-rich mixtures via the biogas dry reforming reaction: Influence of the synthesis method [Internet]. ResearchGate. [cited 2018 May 26]. Available from: https://www.researchgate.net/publication/276857677_Nickel_on_alumina_catalysts_for_the_production_of_hydrogen_rich_mixtures_via_the_biogas_dry_reforming_reaction_Influence_of_the_synthesis_method

51. Nagaoka K, Seshan K, Lercher JA, Aika K. Activation mechanism of methane-derived coke (CHx) by CO2 during dry reforming of methane – comparison for Pt/Al2O3 and Pt/ZrO2. Catal Lett. 2000 Dec 1;70(3–4):109–16.

52. Production of a Hydrogen-enriched Syngas by Combined CO 2 -Steam Reforming of Methane over Co-based Catalysts Supported on Alumina Modified with Zirconia [Internet]. ResearchGate. [cited 2018 May 29]. Available from: https://www.researchgate.net/publication/318367505_Production_of_a_Hydrogen-enriched_Syngas_by_Combined_CO_2_-Steam_Reforming_of_Methane_over_Co-based_Catalysts_Supported_on_Alumina_Modified_with_Zirconia

53. Ni/M-Al 2 O 3 (M=Sm, Ce or Mg) for combined steam and CO 2 reforming of CH 4 from coke oven gas [Internet]. ResearchGate. [cited 2018 May 29]. Available from: https://www.researchgate.net/publication/318709592_NiM-Al_2_O_3_MSm_Ce_or_Mg_for_combined_steam_and_CO_2_reforming_of_CH_4_from_coke_oven_gas

54. COMBINED STEAM AND CO2 REFORMING OF CH4 OVER NICKEL CATALYSTS BASED ON Al2O3-MgO [Internet]. ResearchGate. [cited 2018 May 29]. Available from: https://www.researchgate.net/publication/316350780_COMBINED_STEAM_AND_CO2_REFORMING_OF_CH4_OVER_NICKEL_CATALYSTS_BASED_ON_Al2O3-MgO

55. Jang W-J, Jeong D-W, Shim J-O, Kim H-M, Roh H-S, Son IH, et al. Combined steam and carbon dioxide reforming of methane and side reactions: Thermodynamic equilibrium analysis and experimental application. Appl Energy. 2016;173(C):80–91.

56. Lee HY, Kim AR, Park M-J, Jo JM, Lee DH, Bae JW. Combined steam and CO2 reforming of CH4 using coke oven gas on nickel-based catalyst: Effects of organic acids to nickel dispersion and activity. Chem Eng J. 2015;Complete(280):771–81.

57. Olah GA, Goeppert A, Czaun M, Prakash GKS. Bi-reforming of Methane from Any Source with Steam and Carbon Dioxide Exclusively to Metgas (CO–2H2) for Methanol and Hydrocarbon Synthesis. J Am Chem Soc. 2013 Jan 16;135(2):648–50.

58. Steam treatment on Ni/-Al2O3 for enhanced carbon resistance in combined steam and carbon dioxide reforming of methane [Internet]. ResearchGate. [cited 2018 May 29]. Available from: https://www.researchgate.net/publication/237072920_Steam_treatment_on_Ni-Al2O3_for_enhanced_carbon_resistance_in_combined_steam_and_carbon_dioxide_reforming_of_methane

59. Koo KY, Roh H-S, Jung UH, Yoon WL. Combined H2O and CO2 reforming of CH4 over Ce-promoted Ni/Al2O3 catalyst for gas to liquid (GTL) process: Enhancement of Ni–CeO2 interaction. Catal Today. 2012 May 20;185(1):126–30.

60. Dry Reforming Combined With Steam Reforming Of Methane For Hydrogen Production Over Ni/Ceo 2 Catalyst [Internet]. ResearchGate. [cited 2018 May 29]. Available from: https://www.researchgate.net/publication/266483841_Dry_Reforming_Combined_With_Steam_Reforming_Of_Methane_For_Hydrogen_Production_Over_NiCeo_2_Catalyst

61. Baek S-C, Bae J-W, Cheon JY, Jun K-W, Lee K-Y. Combined Steam and Carbon Dioxide Reforming of Methane on Ni/MgAl<Subscript>2</Subscript>O<Subscript>4</Subscript>: Effect of CeO<Subscript>2</Subscript> Promoter to Catalytic Performance. Catal Lett. 2011 Feb 1;141(2):224–34.

62. Koo KY, Roh H-S, Jung UH, Seo DJ, Seo Y-S, Yoon WL. Combined H2O and CO2 reforming of CH4 over nano-sized Ni/MgO-Al2O3 catalysts for synthesis gas production for gas to liquid (GTL): Effect of Mg/Al mixed ratio on coke formation. Catal Today. 2009 Aug 15;146(1):166–71.

63. Koo KY, Roh H-S, Seo YT, Seo DJ, Yoon WL, Park SB. Coke study on MgO-promoted Ni/Al2O3 catalyst in combined H2O and CO2 reforming of methane for gas to liquid (GTL) process. Appl Catal Gen. 2008 Jun 1;340(2):183–90.

64. Dodgson IL. Catalyst Manufacture, 2nd ed by Alvin B. Stiles and Theodore A. Koch Marcel Dekker: New York. 1995. 291 pp. $145. ISBN 0-8247-9430-3. Org Process Res Dev. 2000 Mar 1;4(2):131–2.

65. Copéret C. Synthesis of Solid Catalysts. Edited by Krijn P. de Jong. ChemCatChem. 2010 May 25;2(6):706–706.

66. Carati A, Ferraris G, Guidotti M, Moretti G, Psaro R, Rizzo C. Preparation and characterisation of mesoporous silica-alumina and silica-titania with a narrow pore size distribution. Catal Today. 2003 Jan 15;77(4):315–23.

67. Ghoneim SA, El-Salamony RA, El-Temtamy SA. Review on Innovative Catalytic Reforming of Natural Gas to Syngas. World J Eng Technol. 2016;04(01):116–39.

68. Hagen J, Chorkendorff I, Niemantsverdriet JW, Kinetics, Thomas JM, Thomas WJ, et al. Author. 1998.

69. Regalbuto J. Catalyst Preparation: Science and Engineering. CRC Press; 2016. 490 p.

70. Schmidt F. New catalyst preparation technologies—observed from an industrial viewpoint. Appl Catal Gen. 2001 Nov 30;221(1):15–21.

71. Deutschmann O, Knözinger H, Kochloefl K, Turek T. Heterogeneous Catalysis and Solid Catalysts. In: Ullmann's Encyclopedia of Industrial Chemistry [Internet]. American Cancer Society; 2009 [cited 2018 May 29]. Available from: https://onlinelibrary.wiley.com/doi/abs/10.1002/14356007.a05_313.pub2

72. Hagen J. Industrial Catalysis: A Practical Approach. John Wiley & Sons; 2015. 546 p.

73. HBHetCat.pdf [Internet]. [cited 2018 May 29]. Available from: http://scs.illinois.edu/suslick/documents/HBHetCat.pdf

74. Thomas JM. Handbook Of Heterogeneous Catalysis. 2., completely revised and enlarged Edition. Vol. 1–8. Edited by G. Ertl, H. Knözinger, F. Schüth, and J. Weitkamp. Angew Chem Int Ed. 48(19):3390–1.

75. Handbook of Heterogeneous Catalysis, 8 Volume Set, 2nd Edition [Internet]. Wiley.com. [cited 2018 May 29]. Available from: https://www.wiley.com/en-us/Handbook+of+Heterogeneous+Catalysis%2C+8+Volume+Set%2C+2nd+Edition-p-9783527312412

76. Thomas JM, Thomas WJ. Principles and practice of heterogeneous catalysis [Internet]. Weinheim ; New York : VCH; 1996 [cited 2018 May 29]. Available from: https://trove.nla.gov.au/version/46591365

77. Argyle M, Bartholomew C. Heterogeneous Catalyst Deactivation and Regeneration: A Review. Catalysts. 2015 Feb 26;5(1):145–269.

78. Rostrup-Nielsen JR, Sehested J, Nørskov JK. Hydrogen and synthesis gas by steam- and C02 reforming. In: Advances in Catalysis [Internet]. Academic Press; 2002 [cited 2018 May 31]. p. 65–139. Available from: http://www.sciencedirect.com/science/article/pii/S036005640247006X

79. Rostrup-Nielsen JR. Catalytic Steam Reforming. In: Catalysis [Internet]. Springer, Berlin, Heidelberg; 1984 [cited 2018 Jun 3]. p. 1–117. (Catalysis). Available from: https://link.springer.com/chapter/10.1007/978-3-642-93247-2_1

80. Catalyst-Fouling - 3. Deactivation Methods [Internet]. [cited 2018 Jun 3]. Available from: https://catalyst-fouling.wikispaces.com/3.+Deactivation+Methods

81. Helveg S, Sehested J, Rostrup-Nielsen JR. Whisker carbon in perspective. Catal Today. 2011 Dec 15;178(1):42–6.

82. Forzatti P, Lietti L. Catalyst Deactivation. Catal Today. 1999 Sep 14;52(2):165–81.

83. Bartholomew CH. Sintering Kinetics of Supported Metals: Perspectives from a Generalized Power-Law Approach. In: Delmon B, Froment GF, editors. Studies in Surface Science and Catalysis [Internet]. Elsevier; 1994 [cited 2018 May 29]. p. 1–18. (Catalyst Deactivation 1994; vol. 88). Available from: http://www.sciencedirect.com/science/article/pii/S0167299108627263

84. ChemInform Abstract: High Throughput Technology: Approaches of Research in Homogeneous and Heterogeneous Catalysis [Internet]. ResearchGate. [cited 2018 May 30]. Available from: https://www.researchgate.net/publication/265911847_ChemInform_Abstract_High_Throughput_Technology_Approaches_of_Research_in_Homogeneous_and_Heterogeneous_Catalysis

85. X-ray Powder Diffraction (XRD) [Internet]. Techniques. [cited 2018 May 30]. Available from: https://serc.carleton.edu/research_education/geochemsheets/techniques/XRD.html

86. [cited 2018 Jun 4]. Available from: http://nptel.ac.in/courses/103103026/13

87. X-Ray Diffraction – XRD – Particle Analytical [Internet]. [cited 2018 May 30]. Available from: http://particle.dk/methods-analytical-laboratory/xrd-analysis/

88. Venezia AM. X-ray photoelectron spectroscopy (XPS) for catalysts characterization. Catal Today. 2003 Jan 15;77(4):359–70.

89. Crystallography: past and present | SpringerLink [Internet]. [cited 2018 May 30]. Available from: https://link.springer.com/article/10.1007/s00339-007-4223-2

90. BET – Particle Analytical [Internet]. [cited 2018 May 30]. Available from: http://particle.dk/methods-analytical-laboratory/surface-area-bet-2/

91. BET Surface Area & Pore Volume Analyzer [Internet]. [cited 2018 May 30]. Available from: https://www.iitk.ac.in/dordold/index.php?option=com_content&view=category&layout=blog&id=223&Itemid=242

92. Leofanti G, Padovan M, Tozzola G, Venturelli B. Surface area and pore texture of catalysts. Catal Today. 1998 May 28;41(1):207–19.

93. Reaction Rates and Selectivity in Catalyst Pores - ScienceDirect [Internet]. [cited 2018 May 30]. Available from: https://www.sciencedirect.com/science/article/pii/S0360056408601091

94. Adsorption of Gases in Multimolecular Layers - Journal of the American Chemical Society (ACS Publications) [Internet]. [cited 2018 May 30]. Available from: https://pubs.acs.org/doi/abs/10.1021/ja01269a023

95. Haber J, Block JH, Delmon B. Manual of methods and procedures for catalyst characterization (Technical Report). Pure Appl Chem. 1995;67(8):1257–306.

96. Pennycook SJ, Chisholm MF, Lupini AR, Varela M, Borisevich AY, Oxley MP, et al. Aberration-corrected scanning transmission electron microscopy: from atomic imaging and analysis to solving energy problems. Philos Trans R Soc Lond Math Phys Eng Sci. 2009 Sep 28;367(1903):3709–33.

97. [cited 2018 Jun 4]. Available from: http://nptel.ac.in/courses/103103026/15

98. Syngas Production from Natural Gas Using ZrO2-Supported Metals [Internet]. ResearchGate. [cited 2018 Jun 1]. Available from: https://www.researchgate.net/publication/222083827_Syngas_Production_from_Natural_Gas_Using_ZrO2-Supported_Metals

99. Li Y, Wang Y, Zhang X, Mi Z. Thermodynamic analysis of autothermal steam and CO2 reforming of methane. Int J Hydrogen Energy. 2008 May 1;33(10):2507–14.

100. Thermodynamic Analyses of Tri-reforming Reactions To Produce Syngas - Energy & Fuels (ACS Publications) [Internet]. [cited 2018 May 29]. Available from: https://pubs.acs.org/doi/abs/10.1021/ef500084m

101. Thermodynamic equilibrium analysis of combined carbon dioxide reforming with partial oxidation of methane to syngas [Internet]. ResearchGate. [cited 2018 Jun 2]. Available from: https://www.researchgate.net/publication/221955819_Thermodynamic_equilibrium_analysis_of_combined_carbon_dioxide_reforming_with_partial_oxidation_of_methane_to_syngas

102. On the coke deposition in dry reforming of methane at elevated pressures [Internet]. ResearchGate. [cited 2018 Jun 2]. Available from: https://www.researchgate.net/publication/273390619_On_the_coke_deposition_in_dry_reforming_of_methane_at_elevated_pressures

103. Optimization of steam methane reforming coupled with pressure swing adsorption hydrogen production process by heat integration [Internet]. ResearchGate. [cited 2018 Jun 2]. Available from: https://www.researchgate.net/publication/277338101_Optimization_of_steam_methane_reforming_coupled_with_pressure_swing_adsorption_hydrogen_production_process_by_heat_integration

104. Thermodynamic and kinetic analyses for hydrogen production via methane autothermal reforming [Internet]. ResearchGate. [cited 2018 Jun 2]. Available from: https://www.researchgate.net/publication/286203515_Thermodynamic_and_kinetic_analyses_for_hydrogen_production_via_methane_autothermal_reforming

105. Reforming of CH4 by Partial Oxidation: Thermodynamic and Kinetic Analyses [Internet]. ResearchGate. [cited 2018 Jun 2]. Available from: https://www.researchgate.net/publication/247375781_Reforming_of_CH4_by_Partial_Oxidation_Thermodynamic_and_Kinetic_Analyses

106. Le Chatelier’s Principle [Internet]. [cited 2018 May 31]. Available from: https://www.chemguide.co.uk/physical/equilibria/lechatelier.html

107. Thermodynamic Analyses of Tri-reforming Reactions To Produce Syngas - Energy & Fuels (ACS Publications) [Internet]. [cited 2018 May 29]. Available from: https://pubs.acs.org/doi/10.1021/ef500084m

108. Le Chatelier’s principle [Internet]. [cited 2018 May 30]. Available from: https://www.khanacademy.org/science/chemistry/chemical-equilibrium/factors-that-affect-chemical-equilibrium/v/le-chatelier-s-principle